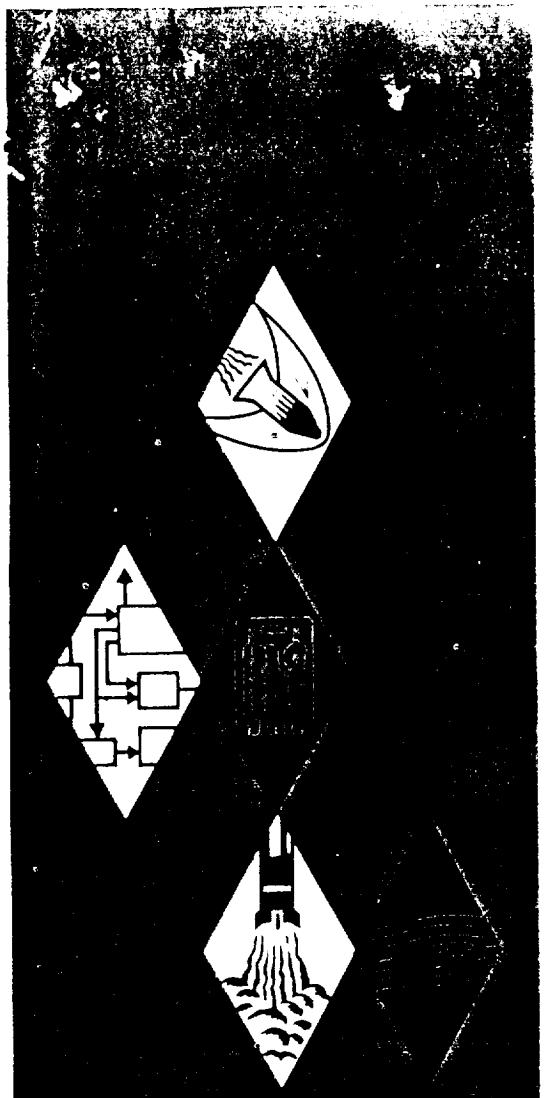

RESEARCH
ENGINEERING
PRODUCTION

AEROSPACE RESEARCH • AERODYNAMICS • PROPULSION • STRUCTURAL DYNAMICS • ELECTRONIC SYSTEMS AND INSTRUMENTS • COMPUTER MODULES

MIXING PROCESSES IN SUPERSONIC COMBUSTION

BY

A. FERRI, G. MORETTI & SL. SLUTSKY

GENERAL APPLIED SCIENCE LABORATORIES, INC.

MERRICK and STEWART AVENUES, WESTBURY, L.I., N.Y. · (516) ED 3-6960

MIXING PROCESSES IN SUPERSONIC COMBUSTION*

Antonio Ferri[1,2], Gino Moretti[2], and Simon Slutsky[2]

1. Introduction. In the latter years of his scientific activity, Prof. von Karman was greatly interested in the field of fluidynamics associated with chemical reactions, which he described with the word aerothermochemistry. In honoring him today, we feel it appropriate to present here some work in this field performed by a group of scientists, who worked following his inspiration under the direction of the senior author. The work was performed at the General Applied Science Laboratories, Inc., of which he had been one of the founders and with which he had been associated. The specific problem discussed here had always been of great interest to him because of his strong belief in the necessity of utilizing vehicles with air-breathing engines for hypersonic flight and for the first stages of launching of space vehicles.

The problem of burning in a stream moving at supersonic speeds is of practical interest for the design of ram engines moving at hypersonic velocity because supersonic combustion simplifies the aerodynamic and structural design of the engine.

Consider schematically a classical ramjet engine as shown in

The work presented here has been supported in part by the following contracts: A. F. Office of Scientific Research, AF-49(638)-991, Contract Off. Dr. B. Wolfson; Air Systems Div., WPAFB, AF-33(657)-10463, Contract Off. Lt. R. Crossley; NASA, G.C. Marshall Space Flight Center, NAS 8-2686, Contract Off. Mr. W. Dahm. The authors wish to acknowledge the contributions of Messrs. D. Magnus, G. Bleich and J. Tamagno to the material presented herein.

(1) New York University, New York, N. Y.
(2) General Applied Science Laboratories, Inc., Westbury, New York.

Figure 1. The engine is composed of an inlet that decelerates the air to subsonic velocity. Fuel is added to the stream in the burner. There the static temperature of the air increases. The expansion of the stream in the nozzle produces high velocities and therefore thrust.

As the flight Mach number increases the performance of such an engine deteriorates; the efficiency of the inlet decreases (because of shock losses, and at the same time the static temperature in the burner before combustion rapidly increases. Under these conditions the addition of fuel in the burner produces small changes and even possible reductions in the temperature of the air because of formation of intermediate reaction products such as atoms and free radicals which cannot recombine at this high temperature. As a consequence, the largest part of the heat release does not occur in the burner but in the nozzle, during the expansion process. In Fig. 2, a typical variation of the static temperature of the air as a function of Mach number before combustion is given for equilibrium conditions. This figure also illustrates the strong decrease in engine efficiency as evidenced by the behavior of the specific impulse (thrust per unit weight of fuel) obtainable with the subsonic engine.

The structural problems related to such an engine design also become extremely complex because of the large heat transfer in the burner region due to the high static pressure and because the area of the minimum sections of the nozzle and inlet must be varied as a function of the Mach number.

A careful study of the problem indicates that the subsonic approach does not appear promising for hypersonic flight. Several different approaches have been suggested for ramjets using combustion occurring in a supersonic flow field. One approach that appears quite promising is that by the senior author suggested in Ref. 1 utilizing diffusive mixing as a control mechanism for combustion of two reacting streams moving supersonically in the same general direction (Fig. 3). One stream consists of air, the other of gaseous fuel; the two streams mix and react. If the reaction is fast and the losses due to mixing are small then it is found that the system can be very efficient at high Mach numbers. In order to obtain fast reaction the free stream air must be decelerated to lower supersonic speeds so that the static temperature of the air in the mixing region is increased sufficiently. The deceleration is accomplished by means of an inlet. However, in this scheme the most important determining parameter is the static temperature of the air and not the Mach numoer at the burner; therefore, a constant geometry inlet with fixed contraction ratio can be used because as the flight Mach number increases, the Mach number at the burner station required to maintain the ignition temperature necessary for reliable combustion also increases. In order to minimize mixing losses, the fuel is injected tangentially to the stream, and at high velocity. A very convenient fuel for this application is hydrogen because of its high specific impulse as

as well as because of its attractive cooling capabilities. However, other fuels can be utilized for various specific applications.

The mixing of the two high velocity streams of fuel and air must occur in a short time. If the pressure and temperature at the mixing region is sufficiently high, the mixture reacts almost instantaneously. After combustion the flow is expanded in a nozzle in which the flow remains supersonic throughout. The time available for reaction in practical burner lengths is of the order of 10^{-4} to 10^{-5} seconds because in the hypersonic flight regime the gases in the engine move at velocities of the order of 10^4 ft/sec. Simple fixed geometry engines which have very attractive performance capability can be designed based on such requirements. Typical engine performance attainable on the basis of a cycle analysis for a fixed geometry engine are shown in Figures 4 and 5 (taken from Reference 2). Figure 4 gives the flow properties at the burner region for the engine as a function of Mach number. Figure 5 gives the specific impulse of the fuel and of the air. This engine scheme promises future maximum specific impulses of the order of 2000 sec. This is almost as good as that obtainable with chemical rocket engines. A detailed discussion of the problems related to the engine design and of the practical possibility of such a configuration has been given in Ref. 1 and a more up-to-date analysis of such problems is presented in the Seventh Lanchester Lecture delived tomorrow in London,

by the senior author (Ref. 2). In this paper some of the analytical approaches developed in relation to the fluidynamic and chemical problems will be reviewed in some detail.

2. Combustion Processes Controlled by Mixing. In the mixing process of two streams moving in a parallel direction, various transport mechanisms take place, including diffusion of species, conduction of heat and exchange of momentum between the two fluids. Either the mass diffusion process or the thermal diffusion process associated with mixing can be used in order to generate a stable combustion process. These two different mechanisms for controlling combustion each have practical interest, with application, however, to different speed ranges. The diffusion of species is a more suitable mechansim for obtaining efficient combustion control at high flight Mach numbers, whereas the thermal transport can be used to control combustion in the lower range of flight Mach number or when the chemical reactions are slow.

In order to clarify the difference between the two controlling processes consider a jet of a gas discharging into the flow of a different gas moving at supersonic speed (Fig. 6). For the high values of flight Mach number, one of the streams will be "pure" air which has been decelerated to lower Mach number and therefore has high static temperature, while the second is gaseous fuel also at high temperature, possibly because it has been used for cooling the structure. The mixing of the two gases is gradual. Because of the high static temperature in the mixing

region and the large consequent reaction rates, combustion takes place very rapidly. For practical values of static pressure and temperature, the mass diffusive mixing process is much slower than the reaction process; therefore the mixing is the controlling mechanism for the heat release. A requirement for such a combustion process is that the air stream be decelerated to sufficiently lower (but still supersonic) Mach number and high static temperature so that the reactions become very fast. The combustion length in this case is then determined by the mixing length.

At lower flight Mach numbers, the maximum static temperature that can be reached by decelerating the air stream is not sufficiently high to produce high reaction rates. Therefore, such a mechanism is not satisfactory unless the fuel is at much higher temperature than the air. In this case, heat transport can be used for the combustion control. As an example of combustion control by thermal transport we can consider a stream of a premixed combustible gas, such as air and hydrogen, and assume that a small pilot jet of precombusted gas having very high static temperature of the fuel mixture. Because of this high local temperature, reaction is initiated. Heat is produced locally that tends to balance the cooling on the boundaries of the pilot flame caused by the mixing process. If the heat produced by the reaction is large enough to at least balance the cooling produced by mixing, then the combustion continues and the flame extends into the premixed gas.

Examples of the two different types of combustion are indicated in Figures 6 and 7. Figure 6a indicates schematically the geometry of the

apparatus and the flame shape. The air temperature of the external stream in this case is sufficiently high to start combustion. The static temperature increases rapidly and combustion takes place as soon as mixing occurs. Figure 6b is a photograph of the flame obtained experimentally for this case. The experiments are taken from Reference 3. Figure 7a indicates schematically the geometry and the flame shape for the second case. In this case, the central jet has very high temperatures. The central jet has been obtained by combusting fuel with an oxidizer at subsonic speed. The external flow is cold, however the flame continues because of the local heat release at the mixing zone. Figure 7b shows a photograph of a flame obtained experimentally for this condition at GASL.

This second process is of interest because it indicates that supersonic combustion can be generated also when the static temperature is low and can be controlled by a mixing process. Furthermore, this scheme can be useful when the reaction rates are small as in the case of hydrocarbon combustion processes.

3. Qualitative Description of the Mixing Process in Presence of Chemical Reaction. The problem of the mixing of two reacting gases is extremely complex because of the many fluidynamic and chemical parameters involved. The simplest possible case that can be considered is when the process is approximately two-dimensional or axially symmetric, and this case is indicated schematically in Figure 8. A jet of gaseous fuel is injected in a stream of air moving at supersonic speed. The velocity vectors, V_1 and V_2 of the

air and of the fuels are different but have approximately the same direction. The static pressures at the exit are equal and the static temperature T_1 and T_2 are different. The line a - a of Figure 8 is either a plane of symmetry or an axis of symmetry or a wall. The two gases mix. Several regions of the flow can be defined; the line AA divides the region in which the fluid is air (region 1) from the region 2 where the fluid contains the elements nitrogen, oxygen, and hydrogen. Line AB further divides the region in which the fluid is pure hydrogen from the region 2 where a mixture exists.

For this simple mixing problem two limiting cases can be considered analytically, the first limiting case corresponds to the assumption that the two gases do not react. Then the process is a pure mixing process that can be analyzed on the basis of mixing theories using boundary layer types of equations. In such an analysis, if the mixing is of laminar type, the analysis can be performed either numerically without necessity of additional simplifications or analytically by simplifying the description of the transport properties. If the mixing is turbulent, then information concerning the transport properties must be obtained from additional experimental studies. The analysis of this type of problem requires substantial extension of existing methods because of the low molecular weight of the hydrogen which affects the transport properties. Use of classical types of analysis which employ simplified or mixing length theories for representation of the transport properties give unsatisfactory results. The second limiting case corresponds to

the assumption that the gases react immediately, i.e., the reaction rates are infinitely fast. In this case local equilibrium exists so that Mollier diagrams can be used to determine the numerical relationships between pressure, density, temperature, total enthalpy and composition. In this second limiting case, additional regions and an additional line can be defined in the flow called the "flame sheet" (line AD of Fig. 9). The flow in region 2a is oxygen rich, containing only water vapor, oxygen and nitrogen whereas in region 2b the gas is hydrogen rich, and contains water vapor, nitrogen and hydrogen. Consequently the remaining concern is only with the adequate description of the mixing process. However, it must be noted that in the usual mixing type of analysis, using boundary layer types of equations a required assumption is that the pressure does not change strongly in the direction normal to the streamlines. This is not necessarily the case in a combustion process where large variations of density occur locally. Such variations of density are concentrated in the region of large heat release and produce large deviations of streamlines and therefore variations of pressure. The pressure disturbances travel approximately along Mach waves of the flow. Therefore the assumption introduced in the boundary layer type of analysis is not justified.

In the case of chemical equilibrium, the pressure variation influences the transport properties and changes the mixture composition and therefore, the assumption of constant pressure at any given cross section can be misleading. In addition the process of combustion in a confined flow is quite different from the simplified picture of free mixing considered above,

because of the presence of the burner walls. Two different sets of modifications must be introduced in the analysis in order to obtain correct information on the actual behavior of the flame.

(i) finite rates of chemical reaction must be considered,

(ii) the assumption of constant static pressure in the normal direction to the stream must be removed, and the effect of external boundary conditions must be introduced.

The first set of modifications imposes severe complications on the numerical analysis. First the various chemical reactions important for the combustion process must be defined. Then the chemical reaction rates must be obtained experimentally. Then an analytical procedure must be established, where the local composition of different species is determined from the finite rate chemical process and not on the basis of local equilibrium properties taken from a Mollier diagram.

The second set of modifications is required when combustion in a duct is considered as schematized in Figure 10. The non-zero angularity of the injection system, the pressure gradients generated by the mixing and combustion processes and the presence of external walls, require that the propagation of pressure disturbances in the presence of the mixing process be considered. Such an approach is somewhat new since viscous problems are traditionally analyzed by using a boundary layer type of approximation. The introduction of finite rate chemistry and of non-uniform pressure distributions imposes such a large complication on the analysis that it becomes mandatory at this stage of the problem to use numerical

procedures for the investigation.

In the following sections some of the procedures developed in connection with the foregoing concepts will be described. Since the combined effects of multi-dimensional aerodynamics, diffusion processes and finite rate chemistry must be treated, a tremendous expenditure of computing time may be anticipated unless special computing methods are devised. Some new approaches suited to this type of problem which eliminates numerical instabilities in the calculations due to finite rate chemistry will be described. Three principal steps related to the numerical procedures had to be taken and will be discussed here. The first step is related to the description of finite rate chemical reactions. In this phase of the analysis the assumption can be introduced that the concentration of elements does not change along any given stream line, so that mixing processes can be ignored.

In the second step the above one dimensional chemistry is combined with mixing using a boundary layer type of analysis.

In the third step two-dimensional or axially symmetric combustion processes are considered which take place within rigid boundaries and with large pressure gradients.

Step One: One-Dimensional Finite Rate Chemistry. In this section we wish to discuss the nature of the chemical system in the absence of mixing or diffusion effects. The basic concepts governing this idealized case

are the conservation of species, momentum and energy written, respectively (Ref. 4, 5, 6)

$$(1) \qquad \frac{da_i}{dt} = u \frac{da_i}{ds} = \frac{W_i \dot{\gamma}_i}{\rho} \qquad i = 1 \ldots N$$

$$(2) \qquad \rho \frac{du}{dt} = \rho u \frac{du}{ds} = - \frac{dp}{ds}$$

$$(3) \qquad \frac{dH}{dt} = u \frac{dH}{ds} = 0$$

where ρ is the mixture density, u the mean (mass) velocity, H the total enthalpy, p the pressure, a_i the mass fraction of the i-th species and $\dot{\gamma}_i$ the chemical rate of production of the i-th species in moles/sec-vol. The total enthalpy is constant by Eq. 3 and is further defined by

$$(4) \qquad H = \frac{u^2}{2} + \sum_{i=1}^{N} a_i h_i = \text{const}$$

where h_i is the partial enthalpy of the i-th species. If we describe the m-th chemical reaction involving reactant species R_i in the general form

$$(5) \qquad \sum_{i=1}^{N} \nu'_{mi} R_i \underset{b_m}{\overset{f_m}{\rightleftharpoons}} \sum_{i=1}^{N} \nu''_{mi} R_i$$

then the rate of formation $\dot{\gamma}_i$ due to the m-th reaction can be written

$$(6) \qquad \dot{\gamma}_{mi} = (\nu''_{mi} - \nu'_{mi}) \left(f_m \prod_j y_j^{\nu'_{mj}} - b_m \prod_j y_j^{\nu''_{mj}} \right)$$

where y_i is the concentration (moles/unit vol.) of the i-th species, ν'_{mi} and ν''_{mi} are either zero or positive integers and the factors f_m and b_m, the forward and backward reaction rates are functions of temperature only. Then

$$(7) \qquad \dot{\gamma}_i = \sum_m \dot{\gamma}_{mi} = F_i (T, y_1, y_2, \ldots y_N)$$

The mass fraction a_i and mole concentration y_i are related by

$$(8) \qquad a_i = \frac{y_i W_i}{\rho}$$

where W_i is the molecular weight.

In addition to the conservation equations the gas mixture obeys the equation of state which can be written

$$(9) \qquad p = R\,T\,Y$$

where

$$Y = \sum_{i=1}^{N} y_i = \rho \sum \frac{\alpha_i}{W_i} = \frac{\rho}{W}$$

Furthermore, there exist L linear relationships among the species concentrations corresponding to the constancy of each of the L element mass fractions.

As seen from the above Eq. 5 it is necessary to have detailed information concerning the nature of the chemical reaction steps and of all the reaction rate constants appearing in the chemical generation described by Eq. 6. As mentioned earlier, this is in general a very difficult task for the physical chemist. It is therefore very fortunate that in the case of the hydrogen-air reaction which is of great interest in hypersonic engine technology, the chemistry and rate kinetics are known in sufficient detail to meet the needs at hand. It has been found that eight forward and eight backward reactions involving six reacting species plus nitrogen as an inert gas describe the essential mechanism at the temperatures of interest. These are listed as follows:

$$(10) \qquad 1. \quad H + O_2 \underset{b}{\overset{f}{\rightleftharpoons}} OH + O$$

(11) 2. $O + H_2 \rightleftharpoons OH + H$

(12) 3. $H_2 + OH \rightleftharpoons H + H_2O$

(13) 4. $2OH \rightleftharpoons O + H_2O$

(14) 5. $H_2 + M \rightleftharpoons 2H + M$

(15) 6. $H_2O + M \rightleftharpoons OH + H + M$

(16) 7. $OH + M \rightleftharpoons O + H + M$

(17) 8. $O_2 + M \rightleftharpoons 2O + M$

where M is any species acting as a third body. The seven species H, O, H_2O, OH, O_2, H_2 and N_2 are numbered respectively from 1 to 7 and for lack of better information, the concentration of M is considered to be equal to the sum of all seven of the species concentrations.

The corresponding reaction rate coefficients were estimated (Ref. 6, 7) as follows:

(18)
$$f_1 = 3 \times 10^{14} e^{-8810/T}$$
$$f_2 = 3 \times 10^{14} e^{-4030/T}$$
$$f_3 = 3 \times 10^{14} e^{-3020/T}$$
$$f_4 = 3 \times 10^{14} e^{-3020/T}$$
$$f_5 = 20.8 \times 10^{19} T^{-1} e^{-54,000/T}$$
$$f_6 = 30.6 \times 10^{21} T^{-1} e^{-62,200/T}$$
$$f_7 = 25.3 \times 10^{19} T^{-1} e^{-52,000/T}$$
$$f_8 = 2.9 \times 10^{19} T^{-1} e^{-60,600/T}$$

$$b_1 = 4 \times 10^{14} e^{-9030/T}$$

$$b_2 = 3 \times 10^{14} e^{-3030/T}$$

$$b_3 = 3 \times 10^{14} e^{-1260/T}$$

$$b_4 = 3 \times 10^{14} e^{-1260/T}$$

(18) (cont'd)

$$b_5 = 10^{21} T^{-1.5} e^{-52,000/T}$$

$$b_6 = 10^{23} T^{-1.5} e^{-58,000/T}$$

$$b_7 = 10^{21} T^{-1.5} e^{-51,000/T}$$

$$b_8 = 1.4 \times 10^{25} T^{-2.5} e^{-59,600/T}$$

T is the absolute temperature in degrees Kelvin. The rates f_1-f_8 and b_1-b_4 are in units of $cm^3/mole\ sec$ while b_5-b_8 are in $cm^6/mole^2 sec$.

The integration of the above system of equations is a simple matter on large scale digital computers and was carried out for one-dimensional flows at a number of organizations during the recent years (Ref. 8). It was noticed during these calculations that the step sizes imposed by the Runge-Kutta and predictor-corrector error control criteria were extremely small even though it appeared that there were negligible chemical changes in the gas stream. Yet, when the step size was increased, violent numerical oscillations of the reactive species, O, H, OH, and H_2O occurred. This behavior of the computations was already well known and was discussed in connection with chemical kinetics problems as long ago as 1952 by Curtiss and Hirschfelder (9) and as recently as 1962 by Hirschfelder (10) as well as many others. Comparison was made in

these references with the "stiff equation" problem occuring in over-controlled servomechanical systems.

The physical basis of the "stiffness" can be somewhat clarified by the following reasoning. It is noted from Equations (10)-(17) that every reaction generating water (y_3) requires the expenditure of OH radicals (y_4) i.e.,

(19) $$\dot{Y}_3 = a_{34}\ y_4 - a_{33}\ y_3$$

where

$$a_{34} = f_3\ y_6 + f_4\ y_4 + b_6\ y_1\ Y$$

$$a_{33} = b_3\ y_1 + b_4\ y_2 + f_6\ Y$$

and the balance of OH is controlled by the equation

(20) $$\dot{Y}_4 = -a_{44}\ y_4 + (\text{sum of the other terms})$$

where

$$a_{44} = a_{34} + b_1\ y_2 + b_2\ y_1 + f_7\ Y$$

Since the concentration of the OH radical (y_4) is always small, and since the rate of production of water in the hydrogen-air reaction is very fast, the coefficient a_{34} of y_4 in Equation (19) must be very large and intrinsically

positive. It is also noted that the coefficient a_{44} of y_4 in Equation (2) is never smaller than a_{34} and is therefore also very large and positive. It was found that during the initial and final stages of the reaction (which are the troublesome regions, a_{44} and the "sum of the other terms" do not vary too rapidly and the Equation (20) can be described qualitatively (though somewhat crudely) by the uncoupled linear equation in which $a = a_{44}$ is very large

(21) $$\dot{y} = -ay + b$$

The solution of the finite difference system approximating this equation has the form

$$y_n = a^n y_0 + \frac{b}{a}(1 - a^n)$$

where

$$a = (1 - a\Delta s) \quad \text{- Euler integration}$$

or

$$a = \left(1 - a\Delta s + \frac{(a\Delta s)^2}{2} - \frac{(a\Delta s)^3}{6} + \frac{(a\Delta s)^4}{24}\right) \text{- Runge Kutta}$$

Aside from any questions of truncation error it can be show that numerical instability will result for absolute values of $a\Delta s$ greater than two and spurious for $a\Delta s$ greater than one. The step size must therefore be bounded by magnitudes of the order of $1/a$ which is a very severe constraint. Exceeding the above type of size limitation has been responsible for meaningless results.

Observance of the limitation (to time increments of the order of 10^{-8} sec) has contributed greatly to the difficulty in application of numerical methods to engineering combustion problems. It is further to be noted that the difficulty of carrying out finite rate calculations in the neighborhood of chemical equilibrium is related to this same problem of stiff equations and small stepsize.

Faced with the urgent need for a practical solution of this dilemma, a very detailed investigation of the nature of the chemical equations in the H_2-air reaction was initiated at GASL, Reference 11. In particular the second named author of this paper proceededby reducing the species continuity equations to fourth order by using element conservation which was used to eliminate O_2 and N_2 so that the remaining equations can be written in terms of the active species H, O, H_2O and OH. It was found by numerical experimentation that the molar rates of formation $\dot{\gamma}_1$ to $\dot{\gamma}_4$ could be divided into three principal groups. These were of the form

$$\dot{Y}_i = A_i + \sum_j B_{ij}\, y_j + \sum_j \sum_k C_{ijk}\, y_j\, y_k \qquad i, j, k = 1\text{-}4$$

where A_i, B_{ij} and C_{ijk} represent slowly varying functions. In the initiation and near equilibrium phases of the reaction (which were the numerically recalcitrant phases) it was found that the third term (the sum of quadratic terms) was several orders of magnitude smaller than the first two contributions. This and the near straight line variation of the mass fractions obtained in Reference 5 when plotted (versus time) on a semilog plot Figure 11, suggested

that the species conservation equations were essentially near-linear with near-constant coefficients and that linearization techniques should be very useful in this system. This linearization was carried out by expanding the products of the concentrations in a Taylor series, retaining only terms of zeroth and first order:

$$y_i\, y_j = y_i^{\circ}\, y_j + y_i\, y_j^{\circ} - y_i^{\circ}\, y_j^{\circ} \tag{22}$$

The conservation of species(Equation 1) can then be written

$$\frac{dy_i}{dt} + y_i\, \delta = C_i + \sum_{j=1}^{q} a_{ij}\, y_j \tag{23}$$

where

$$\delta = \frac{1}{\rho}\,\frac{d\rho}{dt} \tag{24}$$

The expression of the species conservation equation in terms of the concentrations y_i instead of the mass fractions a_i is a convenience because then the c_i and a_{ij} depend only on temperature instead of both temperature and pressure which would be otherwise required. The condensation δ is assumed constant over a single calculation step. For a given step, coefficients c_i and a_{ij} are functions of the initial values of the concentrations y_i° and the temperature T°, which is likewise assumed constant at the initial value for

the step. The coefficients are written out in detail in Reference 11 . Under the above assumptions the system Equation 23 can be solved for a single calculation step.

For a constant or prescribed pressure variation along the flow the velocity is determined by Equation (2) and the temperature from Equation (4), using piecewise parabolic temperature fits to describe the species enthalpies $h_i(T)$.

However, the temperature is also specified by the equation of state, Equation (9) when the pressure is specified. Since these two values of temperature denoted by T(p) and T(h) are not in general equal, a second choice of Δ is made and the solution procedure repeated and the error T(p)-T(h) noted. An interpolation and iteration procedure is then used to minimize the error. The density at the end of the step is then computed from

$$\rho = \sum_{i=1}^{7} y_i \, W_i \tag{25}$$

It will be noted that the system of Equation (23) as defined above is piecewise linear and amenable to many solution techniques other than Runge-Kutta or predictor-corrector.

The first solution procedure used was by determination of the exponential solutions. The problem of stability therefore did not arise. Since the equations actually behave like linear equations with constant coefficients at initiation and near equilibrium, it was not surprising that the solutions were found to extend with accuracy over several orders of magnitude

in a single calculation step in these reaction regions. It was found that the entire reaction could be described with useful accuracy in as little as 10 steps whereas if 40 steps were used (taking 4 seconds on an IBM 7094) the results were practically indistinguishable from the Runge-Kutta, predictor-corrector solutions using about 10,000 steps. It is also significant to note that even with the crudest stepsizes, the asymptotic values of the solutions are correctly reached. Some curves, Figure 12 illustrate this rather well. It will be noted that the permissible stepsize at the beginning and at the end of the reaction (equilibrium) become very large in complete reversal of the requirements of the Runge-Kutta procedure.

The exponential solution technique presents, of course, no difficulties in the hydrogen-air reaction which is reducible to a fourth order system. But GASL is also much concerned with chemical systems such as methane-air combustion which has thirteen species reducible only to nine. The determination of the eigenvalues of the general non-symmetric ninth order matrix is a clumsy, time consuming and not very accurate operation even on the largest available computers. Other numerical solution procedures were therefore examined. Among the integration methods that resulted in stable numerical sequences were the subdomain method, least squares and Galerkin. Undoubtedly others are possible. The subdomain method (Ref. 12) was found to be particularly convenient for numerical application to large order systems.

In order to illuminate the reason that instability was so successfully eliminated by this method it is useful to consider application of the subdomain method to the first order equation (Equation 2) whose stability was considered previously for the Euler and Runge-Kutta solutions.

Using an assumed parabolic variation of concentration with time, substituting the parabola with undetermined coefficients in Equation (21) and setting to zero the integrals of the residue taken between 0 and $\Delta/2$ and between $\Delta/2$ and Δ, enough conditions are satisfied such that successive solutions are related by the difference equation

$$y_{n+1} = y_n\left(1 - \frac{a\Delta}{D_o}\right) + \frac{b\Delta}{D_o} \tag{26}$$

where

$$D_o = \frac{1}{12}\left[3 + (3 - a\Delta)^2\right] > 0$$

This can be integrated;

$$y_n = \alpha^n y_o - \frac{b}{a}(1 - \alpha^n) \tag{27}$$

where

$$\alpha = 1 - \frac{a\Delta}{D_o}$$

The quantity $a\Delta / D_o$ is a positive number lying between zero and .93. It follows that the solution Equation (27) cannot oscillate but instead approaches the correct asymptotic value, b/a.

The extension of the above method to large systems such as the hydrogen and methane oxidation reactions has been carried out successfully. An accurate calculation of a complete hydrogen reaction requires less than 10 seconds of 7094 computer time and the methane reaction takes about 20 to 30 seconds.

Step Two: Coupled Diffusion and Chemical Reaction in Shear Flows. Having eliminated the obstacle of small chemical step size, there remains the problem of coupling the above described technique of chemical computation, which is a one-dimensional process, with shear flow, which is at least two-dimensional. The problem was approached by splitting the species mass fractions into two components, one of which satisfied a portion of the species conservation equation containing the diffusion operator but no chemical generation whereas the other component did the reverse. For purposes of exposition, the conservation equations are written below for a two-dimensional steady boundary layer flow with Lewis and Prandtl numbers equal to unity and the equations are cast in stream function coordinates. (Note that these simplifications were not actually made in the practical case, nor were the equations actually written in these coordinates.)

$$\frac{\partial \alpha_i}{\partial s} = \frac{\partial}{\partial \psi}\left(\rho u \mu \frac{\partial \alpha_i}{\partial \psi}\right) + \frac{w_i \dot{\gamma}_i}{\rho u} \tag{28}$$

$$\frac{\partial H}{\partial s} = \frac{\partial}{\partial \psi}\left(\rho u \mu \frac{\partial H}{\partial \psi}\right) \tag{29}$$

$$\frac{\partial u}{\partial s} = \frac{\partial}{\partial \psi}\left(\rho u \mu \frac{\partial u}{\partial \psi}\right) \tag{30}$$

It is clear that the above equations present no numerical problems in integrating in the case that $\dot{\gamma}_i$ is zero. For $\dot{\gamma}_i$ unequal to zero we define

(31) $$\alpha_i = p_i + q_i$$

and

(32) $$\frac{\partial p_i}{\partial s} = \frac{\partial}{\partial \psi}\left(\rho u \mu \frac{\partial (p_i + q_i)}{\partial \psi}\right)$$

Then in order to satisfy Equation (28), q_i must satisfy

(33) $$\frac{\partial q_i}{\partial s} = \frac{W_i}{\rho u} \dot{\gamma}_i = B_i + \sum_j A_{ij}(p_i + q_i)$$

In the above, $\dot{\gamma}_i$ can be considered linearized and the B_i and A_{ij} coefficients differ from the c_i and a_{ij} of Equation (23) only by including the $W_i/\rho u$ factor.

It is possible to fix the initial conditions for p_i and q_i at the beginning of a computation step in more than one way. In particular, it is possible to assume the combination

(35) $$q_i(x_{n+0}, y_k) = 0$$

$$p_i(x_{n+0}, y_k) = \alpha_i(x_n, y_k)$$

and

$$q_i(x_{n+0}, y_k) = \alpha_i(x_n, y_k)$$

(36)

$$P_i(x_{n+0}, y_k) = 0$$

The subscripts n, k are chosen in anticipation of the finite difference net formulation, and the added zero to n + 0 is required since p and q are in general streamwise discontinuous across a net point although their sum a is continuous.

The choice of initial conditions turns out to be irrelevent for either explicit or implicit computations insofar as numerical stability is concerned.

Consider the explicit formulation with conditions, Equation (35). Then the difference equation corresponding to Equation (32) becomes very simple (the p_i becomes uncoupled) and the solution can be written

$$p_i(n+1, k) = p_i(n, k) + \frac{\Delta s}{(\Delta v)^2} L_k p_i(n, k) \tag{37}$$

where the operator L_k is intended to indicate the vertical shift and summing operator;

$$L_k p_i(n, k) \equiv 1/2 \quad (f_{k+1} + f_k)\, p_i(n, k+1) - (f_{k+1} + 2f_k + f_{k-1})\, p_i(n, k) + (f_k + f_{k-1})\, p_i(n, k-1) \tag{38}$$

Then the solution $a_i(n+1, k)$ term is the change in chemical composition over the diffusion step in which p_i is assumed to remain constant and is calculated from the subdomain chemistry routine as previously described for the equation

$$\frac{\partial}{\partial s}(q_i + p_i(n, k)) = B_i + \sum_j A_{ij}(q_j + p_j(n, k)$$

$$(q_i + p_i(n, k))_o = p_i(n, k) = \alpha_i(n, k) \tag{40}$$

where $\alpha_i(n, k)$ is determined at the (n, k) mesh point. The solution to Equation (40) can then be expressed formally:

$$(41) \qquad q_i(n+1, k) = E_i(n, k) + D_{ij}\,\alpha_j(n, k)$$

It should be noted that p_i need not be kept constant in (40) but can be treated in the subdomain method as a known distribution.

Equation (39) becomes

$$\alpha_i(n+1, k) = M_{ij}\,\alpha_j(n, k) + E_i(n, k)$$

$$M_{ij} = \delta_{ij} + \gamma\,\delta_{ij} L_k + D_{ij}$$

$$\delta_{ij} = \begin{cases} 1 & i = j \\ 0 & i \neq j \end{cases}$$

$$\gamma = \frac{\Delta s}{(\Delta v)^2}$$

For stability the eigenvalues of M must all have absolute value less than one.

In order to examine the stability of this system, the approximation $f_{k+1} = f_k = f_{k-1}$ was made in Equation (38) so that the von Neumann approach is applicable. Then

$$(43) \qquad \gamma L_k \alpha_j(n, k) = -2\gamma f_k (1-\cos\theta)\,\alpha_j(n, k)$$

The stability condition can then be stated

$$-1 < \lambda_D + 1 - 2\gamma f_k (1-\cos\theta) < 1$$

where λ_D is the real part of any eigenvalue of D.

Then

$$\frac{\lambda_D}{2f_k(1-\cos\theta)} < \gamma < \frac{2+\lambda_D}{2f_k(1-\cos\theta)} \tag{44}$$

The lower limit requires that λ_D be negative and the upper limit that

$$\gamma < \frac{2+\lambda_D}{4f_k} \tag{45}$$

and that λ_D be not less than -2, i.e.,

$$-2 < \lambda_D < 0 \tag{46}$$

In order to estimate the eigenvalues of D in an analytic form, we are unfortunately forced again to consider the uncoupled equivalent of Equations(40) and (41). The solution in this case for a two step (parabolic) subdomain technique is

$$q_i(n+1, k) = \frac{A\Delta s}{D_2}\alpha_i(n, k) + \frac{B\Delta s}{D_2} \tag{47}$$

where

$$D_2 = 1/12\left[(3-A\Delta s)^2 + 3\right] \tag{48}$$

so that

$$(49) \qquad -.94 < \lambda_D = \frac{A\,\Delta s}{D_2} < 0$$

This satisfies the requirement (46). For a one-step (linear) subdomain technique, the uncoupled equation gives the same form of solution as (47) except that

$$(50) \qquad D \longrightarrow D_1 = 1 - \frac{A\,\Delta s}{2}$$

and

$$(51) \qquad -2 < \lambda_D = \frac{A\,\Delta s}{D_1} < 0$$

The inequalities of Eq. (51) for the one-step subdomain technique still satisfy Eq. (46) but with all of the approximations made, it is probably a poor risk for coupled diffusion. Just as the eigenvalues of the magnifications matrix depend on the order of the fit, so it also varies somewhat when least squares or Galerkin methods are used.

It can be shown in a similar way that use of Condition (36) results in a completely equivalent step size criteria.

It was furthermore found, on the basis of the same heuristic type of reasoning that the implicit coupled process is unconditionally stable.

We wish to remark at this time that the stability analyses outlined above leave much to be desired from the point of view of exactness or thoroughness. Nevertheless they served their purpose in that they illuminated the landscape into which we were venturing and made it possible

to estimate rather well the order of effort required.

In application of the foregoing to physical problems an axisymmetric configuration was considered, both because of convenience in adapting existing programs, and because of the availability of experimental results with which comparisons were possible and desirable.

Since the flows considered were turbulent the formulation of the conservation equations, for an axisymmetric turbulent flow was based on that of the paper by Zeiberg and Bleich (Ref. 13):

$$(52) \qquad \frac{\partial \alpha_i}{\partial x} = \frac{1}{\upsilon} \frac{\partial}{\partial \psi} \left[\frac{L_e}{\sigma} \frac{\epsilon \rho u y^2}{\upsilon} \frac{\partial \alpha_i}{\partial \psi} \right] + \frac{W_i \dot{\gamma}_i}{\rho u}$$

$$(53) \qquad \frac{\partial u}{\partial x} = - \frac{1}{\rho u} \frac{\partial p}{\partial x} + \frac{1}{\upsilon} \frac{\partial}{\partial \psi} \left[\frac{1}{\upsilon} \epsilon \rho u y^2 \frac{\partial u}{\partial \psi} \right]$$

$$(54) \qquad \overline{C}_p \frac{\partial T}{\partial x} = \frac{1}{\rho} \frac{\partial p}{\partial x} - \frac{1}{\upsilon} \frac{\partial}{\partial \psi} \left[\frac{\overline{C}_p}{\sigma} \frac{1}{\upsilon} \epsilon \rho u y^2 \frac{\partial T}{\partial \psi} \right]$$
$$\frac{\epsilon \rho u y^2}{\upsilon^2} \left[\left(\frac{\partial u}{\partial \psi} \right)^2 + \frac{L_e}{\sigma} \frac{\partial T}{\partial \psi} \sum_i C_{pi} \frac{\partial \alpha_i}{\partial \psi} \right] - \frac{1}{u \rho} \sum_i h_i W_i \dot{\gamma}_i$$

where ψ is the stream function and is related to y by

$$(55) \qquad y^2 = 2 \int_0^{\upsilon} \frac{\upsilon' \, d\upsilon'}{\rho u}$$

In the above, L_e is the turbulent Lewis number, σ the turbulent Prandtl number, $\overline{C}_p$ the mixture specific heat and ϵ the turbulent viscosity. In view of the turbulent nature and the uncertainties of the

mixing in the flow all justification for use of multispecies diffusion coefficients disappears so that a single Lewis number is in order.

The determination of a model to be used for description of the turbulent viscosity is a subject of considerable difficulty, especially for jet flows with large density gradients as occurs in connection with a jet of hydrogen into air. A discussion of the problems involved is presented in Ref. (1) and the results of more recent work will be presented in London (Ref. 2) tomorrow. For the purposes of our combustion studies, we have therefore left open a small black box in our digital computer labeled eddy viscosity into which we pour any model of viscosity that seems appropriate at the moment.

The program was first tried on for size on a 4-inch diameter jet flow which was of some interest in connection with a high-altitude fuel dumping problem. The jet of hydrogen issued at 1038 fps and temperature of 276°K into a hot high-speed exterior stream of air moving at 3069 fps and temperature 1388.5°K. Both streams were assumed at .01 atmosphere pressure.

The viscosity model used in this case was given by

$$\epsilon = .025\, r_{1/2} \left| \rho_e u_e - \rho_j u_j \right| \tag{56}$$

where $r_{1/2}$ is the radius at which ρu is the mean value between $\rho_e u_e$ and $\rho_j u_j$. The resulting calculation (Fig. 13) showed the external stream

first drops in temperature where it mixes with the cold hydrogen and then at a distance of about 4 feet reverses and starts to heat up so that a peak temperature develops at about .25 feet from the axis. The temperature peak then shifts to the axis which has developed a fairly large mass fraction of oxygen (Fig. 14). As burning proceeds this free oxygen then rapidly reacts with the excess hydrogen on the axis.

This calculation has no experimental counterpart available at this time, but was presented because it shows (1) the non-existence of a flame-sheet, and (2) the interesting development of a first temperature peak in the hydrogen-air mixing region.

A second case treated was that of the 0.6-inch diameter hydrogen jet mentioned earlier in connection with mass diffusion control. Here the pressure distribution measured along the axis varies rather strongly both below and above atmospheric pressure. Calculations were made assuming that the static pressure is approximately constant across any cross section of the jet and changes only along the jet. Such calculations made with several different pressure distributions showed strong resulting axial stagnation temperature variations (Fig. 15). The curve computed using a pressure distribution simulating the measured distribution (Fig. 16) showed excellent agreement with the measured axis stagnation temperature. Radial stagnation temperature variations measured at station x = 0.9 ft

also agreed very well with calculated values, (Fig. 17). The flame shape (Fig. 18) was not too well simulated and the complex pressure field may have something to do with this.

The third case considered was of the axisymmetric flame propagation from a pilot flame into a premixed hydrogen-air flow at atmospheric pressure, 300°K and 2100 fps and with equivalence ratio of one. This is the case referred to in connection with combustion control by thermal conduction and diffusion combined with species diffusion. In Fig. 19 we have plotted the calculated isotherms for the flow. It is seen that the pilot first cools but then the temperature rises rapidly along the axis as the premixed gas ignites. The isotherms spread out on parallel cones with a slope of about 10°. This angle is in excellent agreement with the observed angle on the experimental counterpart of this calculation. In Fig. 20 we have further plotted the computed streamlines superimposed upon the isotherms. It will be noted that the streamlines behave very reasonably, curving away from the axis in front of the flame and straightening out in the flame. The streamlines do not become completely straight on the figure because the heat release is not entirely complete. These results seem to indicate very good agreement of the theory with experiment in this type of flame propagation problem.

In a sense Fig. 20 also indicates the limitations of the method of

computation, since the curvature of the streamlines increases indefinitely with distance away from the axis. Such a flow cannot exist at large radial distance without development of pressure gradients.

Step Three: Supersonic Combustion with Pressure Gradients and Mixing. The assumption in the analysis of the combustion that the static pressure is constant at any given section notably simplifies the problem. However, it is not sufficiently accurate for such purposes as the detailed design of combustion chambers because of the large variation of temperature and density produced locally by the reaction, as pointed out in the Introduction.

For the type of process analyzed the chemical reaction produces much larger pressure variations than the diffusive process, and is the main cause of large pressure gradients. In this case, it can be assumed in the analysis that the variation of pressure due to mixing is small compared to the variation of pressure produced by the reaction and can be calculated as a perturbation of a basically inviscid flow. When this assumption is introduced, an approximate analytical method can be developed which takes into account the complex pressure variations due to reactions (Ref. 14). Since these pressure are usually described in terms of a characteristic network, this was taken as the basis for a calculation procedure. We write the exact equations for supersonic flow with diffusion and chemical effects, putting the usual inviscid flow

terms on the left-hand side and the remaining terms on the right-hand side. Such a system can be formally transformed into a system in which differentiation along streamlines and characteristics can be present only in the left-hand side. A formal solution of this system involves (1) the determination of the intersection of characteristics, (2) the solution of the compatibility equation along the characteristics, and (3) the solution of the energy equation along the streamline. Such equations are quasi-linear and therefore can be handled by well-known techniques. The coefficients on the left-hand side of these equations contain the contributions of the inviscid effects only. In a characteristic step such contributions are approximated at the initial points and a first approximation of pressure and enthalpy is made at the intersection of the characteristics. On the basis of this pressure and enthalpy, a better evaluation of the chemical reaction along a streamline is made. The aforementioned coefficients are consequently modified, and the characteristic computation is repeated.

In the two-dimensional case, the momentum equations for the above formulation are:

$$\rho q q_s + p_s = A \tag{57}$$

$$\rho q^2 \theta_s + p_n = 0 \tag{58}$$

where ρ is density, p is pressure, q and θ the modulus and the direction of the velocity relative to engine axis. The quantity A is given by

$$A = (\mu q_n)_n \tag{59}$$

where μ is the viscosity.

The subsequent solution of the compatibility equations requires that A be constant or of small relative variation during an integration step. Then the initial computation can be made approximately using the initially known value A^o, followed by iteration to obtain a more accurate mean value $\overline{A}$.

The continuity equation reads

$$q\rho_s + \rho q_s + \rho q \sigma_n = 0 \tag{60}$$

and the energy equation can be stated (assuming for simplicity that the Lewis and Prandtl numbers are equal to unity)

$$H_s = \frac{1}{\rho q} (\mu H_n)_n \tag{61}$$

where H is the total enthalpy

$$H = h + q^2/2 \tag{62}$$

h being the static enthalpy.

The usual neglect of diffusion along the streamline has been made

in comparison with lateral diffusion.

In order to complete the description of the system we express the enthalpy by means of the equation

$$h_s = \sum_{i=1}^{N} h_i \alpha_{is} + T_s \sum_{i=1}^{N} \alpha_i \frac{d h_i}{dt} \tag{63}$$

where α_i is the mass fraction of species i. From the equation of state we further obtain

$$p_s - \frac{p \rho_s}{\rho} - \frac{p T_s}{T} - R \rho T \sum_i \frac{\alpha_{is}}{W_i} = 0 \tag{64}$$

R being the gas constant and W_i the molecular weight of species i.

The species conservation equations must take into account the mixing of species between streamlines and the change in mass-fraction of the species due to chemical reaction along the streamline. Thus,

$$\alpha_{is} = \frac{1}{\rho q} \frac{\partial}{\partial n} \rho D \frac{\partial \alpha_i}{\partial n} + \frac{\dot{W}_i \gamma_i}{\rho q} \tag{65}$$

where, again for simplicity, a single binary diffusion coefficient D has been assumed. For unit Lewis number we can substitute

$$\rho D = \mu \tag{66}$$

The subsequent algebraic manipulations to put the equations into suitable characteristic form are tedious so that details should be sought in Ref. (14). It is shown that the third equation to be used with Eq. (57)

and (58) can be put in the form

$$(q + \frac{F}{q})q_s + \frac{F}{p} p_s + F\theta_n = E \tag{67}$$

where

$$F = T \sum \alpha_i \frac{dh_i}{dT}$$

$$E = \frac{1}{\rho q}(\mu H_n)_n - \sum_i h_i \alpha_i + \frac{R\rho FT}{p} \sum_i \frac{\alpha_i}{W_i}$$

It is seen that the viscosity does not appear in (57), (58) and (67) except on the right-hand side and so does not directly effect the streamline and characteristic directions and the location of the net intersections.

Conclusion. In conclusion considerable progress has been made in the mathematical treatment of problems involving coupled axis flows, diffusion and chemical reaction. In particular, the mathematical description of multispecies chemical reactions has been very greatly expedited and rendered applicable to two-dimensional flow problems. A number of experiments involving both initially unmixed and premixed hydrogen were available for comparison with calculated results. Agreement in many important respects was excellent.

REFERENCES

(1) A. Ferri, "Possible Directions of Future Research in Air-Breathing Engines", AGARD Combustion and Propulsion Colloquium, Pergamon Press Ltd., London, England, 1960, pp. 3-15.

(2) A. Ferri, "Review of Problems in Application of Supersonic Combustion", Seventh Lanchester Memorial Lecture, Royal Aeronautical Society, London, England, May 14, 1964.

(3) Zakkay, V., and E. Krause, "Mixing Problems with Chemical Reactions", PIBAL Report No. 776, March, 1963.

(4) A. Ferri, P. A. Libby, and V. Zakkay, "Theoretical and Experimental Investigation of Supersonic Combustion", Third ICAS Congress, Stockholm, Sweden, August 27-31, 1962.

(5) P. A. Libby, H. Pergament, M. H. Bloom, "A Theoretical Investigation of Hydrogen-Air Reactions", GASL Technical Report No. 250 (AFOSR 1378), August, 1961.

(6) H. S. Pergament, "A Theoretical Analysis of Non-Equilibrium Hydrogen-Air Reactions in Flow Systems", Paper 63-113, AIAA-ASME Hypersonic Ramjet Conference, April 23-25, 1963.

(7) R. W. Duff, "Calculation of Reaction Profiles Behind Steady State Shock Waves, I. Application to Detonation Waves", J. Chem. Physics, 28, 6, June 1958, pp. 1193-1197.

(8) A. A. Westenberg, and S. Favin, "Complex Chemical Kinetics in Supersonic Nozzle Flow", Ninth International Symposium on Combustion, Cornell University, August, 1962.

(9) C. F. Curtiss and J. O. Hirschfelder, "Integration of Stiff Equations", Proc. N. A. S. 38, 235, 1952.

(10) J. O. Hirschfelder, "Some Remarks on the Theory of Flame Propagation", Ninth International Symposium on Combustion, Cornell University, August, 1962.

(11) G. Moretti, "A New Technique for the Numerical Analysis of Non-Equilibrium Flows", GASL Technical Report No. 412, March, 1964.

(12) S. Crandall, Engineering Analysis, McGraw-Hill Book Company, New York, 1956, p. 147.

(13) S. Zeiberg and G. Bleich, "A Finite-Difference Method Solution of the Laminar Hypersonic, Non-Equilibrium Wake", GASL Technical Report No. 338, February, 1963.

(14) G. Moretti, "Analysis of Two-Dimensional Problems of Supersonic Combustion Controlled by Mixing", Paper presented at AIAA Symposium, New York, January, 1964.

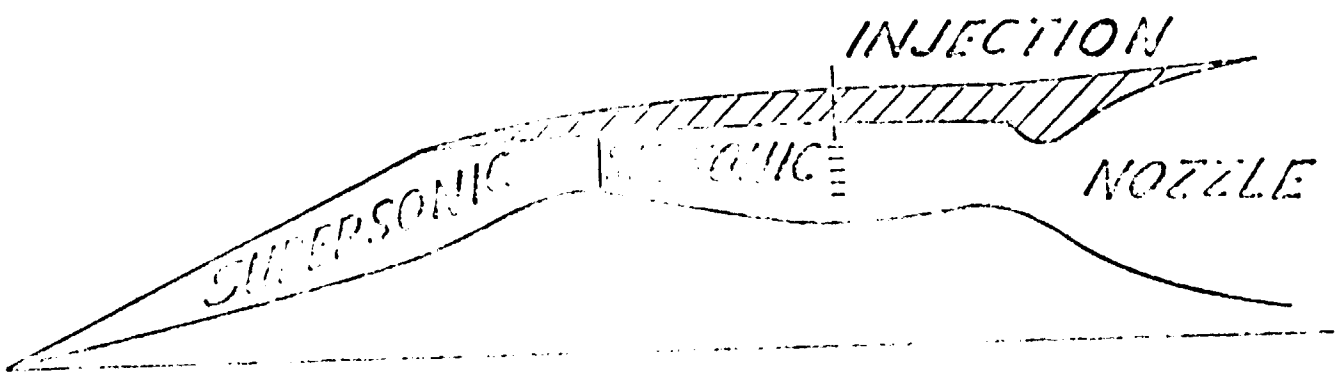

Fig. 1 Schematic of classical ramjet engine

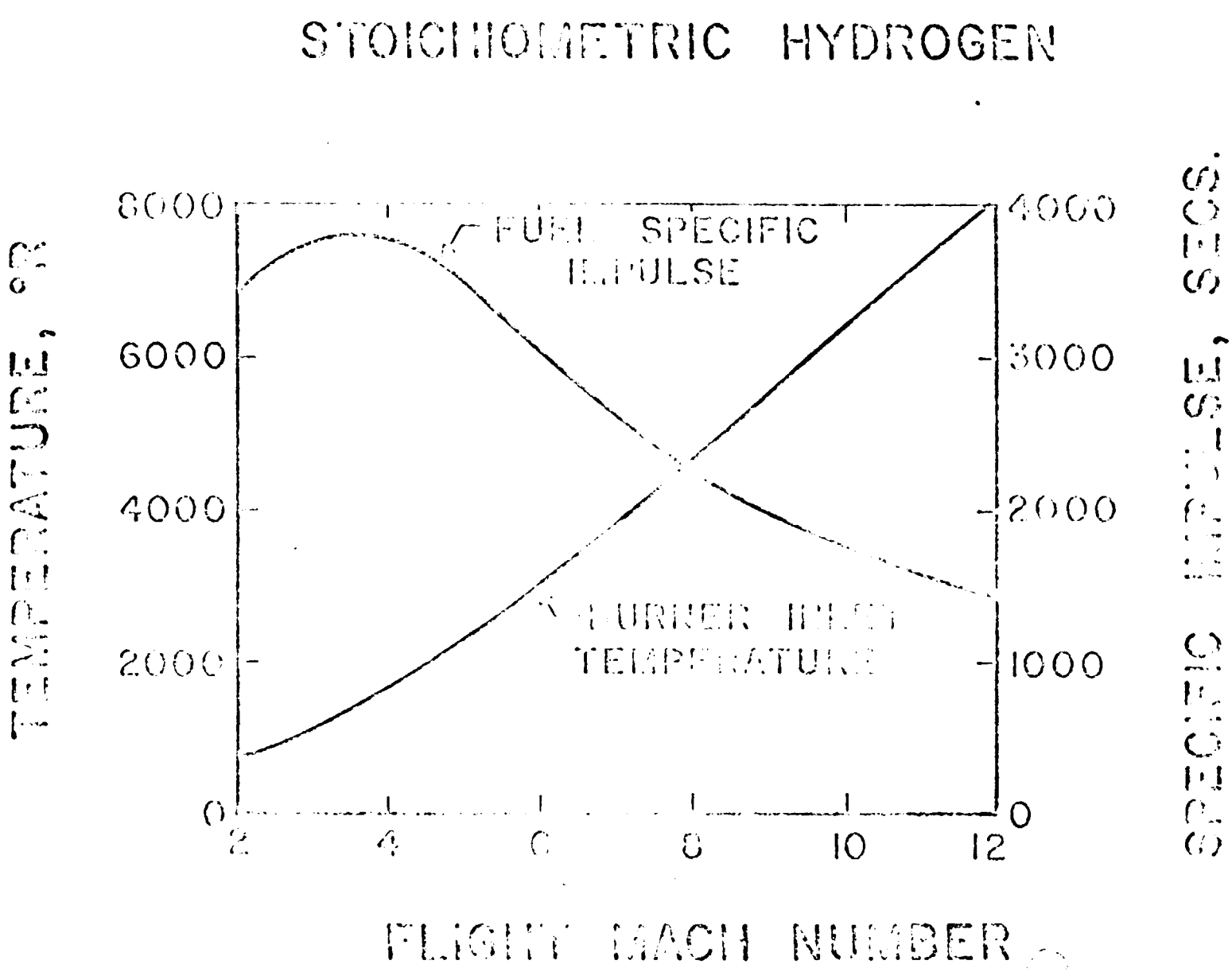

Fig. 2 Typical temperature and impulse variation.

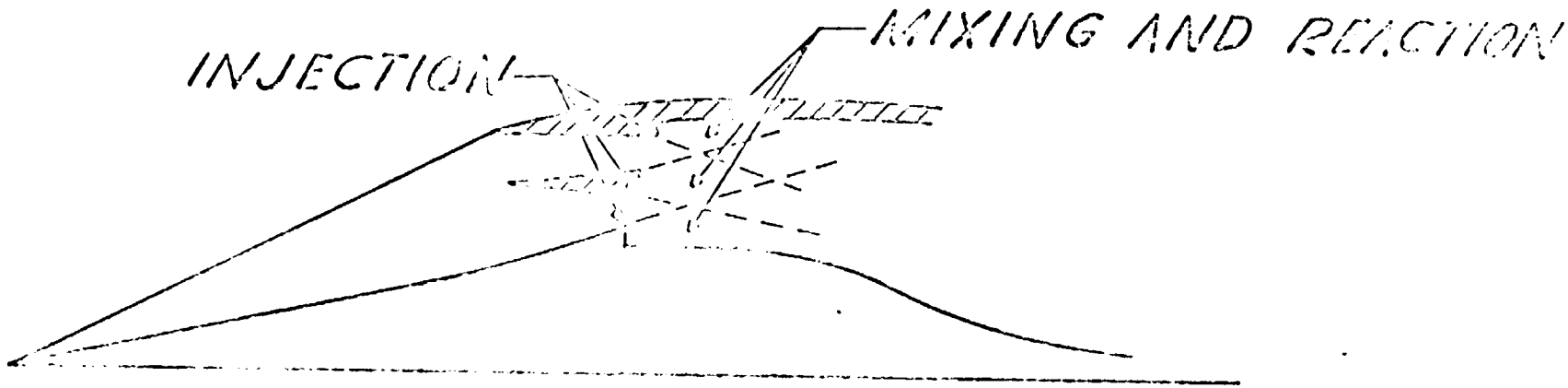

Fig. 3 Schematic of suggested supersonic combustion ramjet

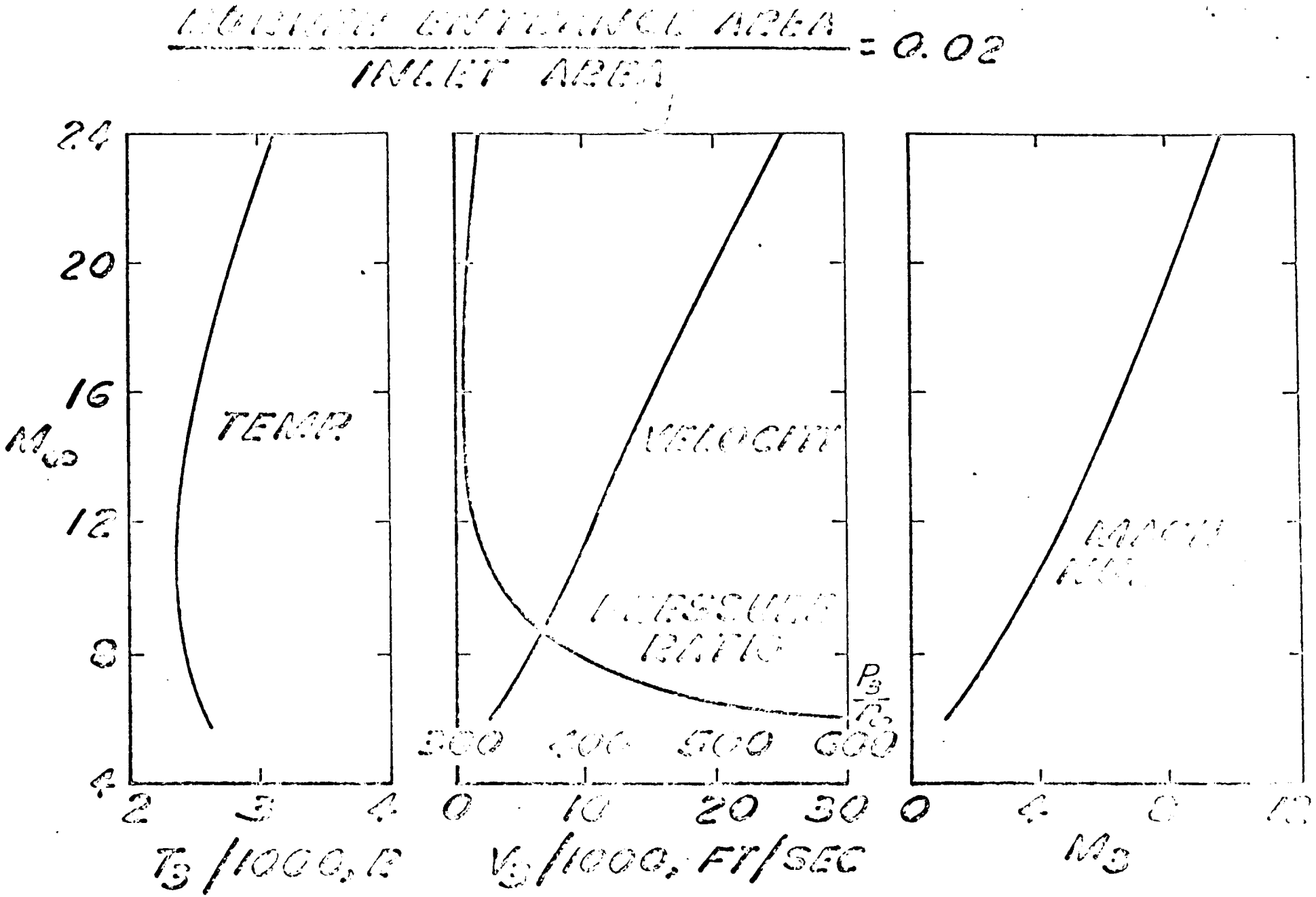

Fig. 4 Flow properties at burner entrance for supersonic combustion ramjet

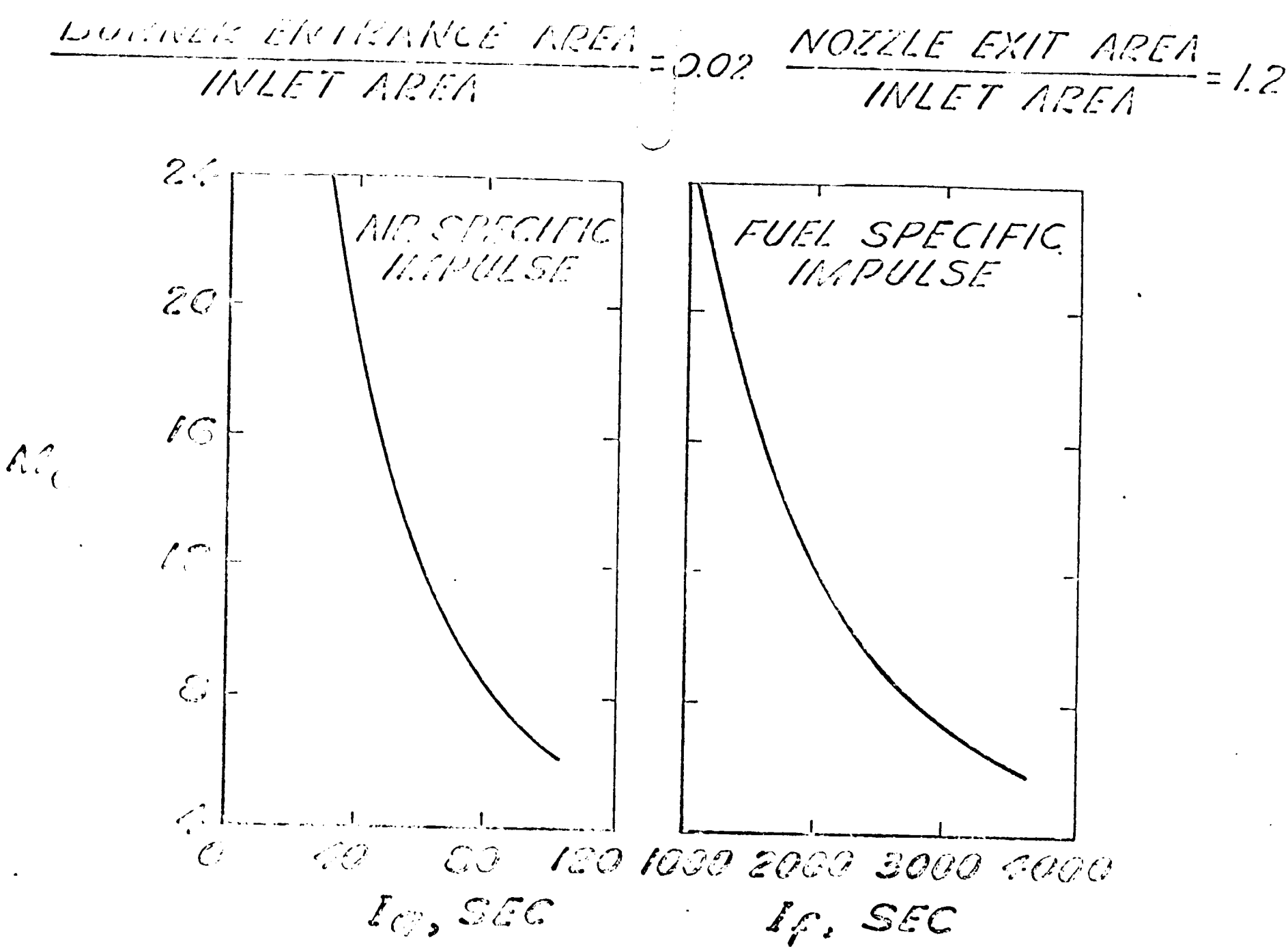

Fig. 5 Specific Impulse of fuel and air

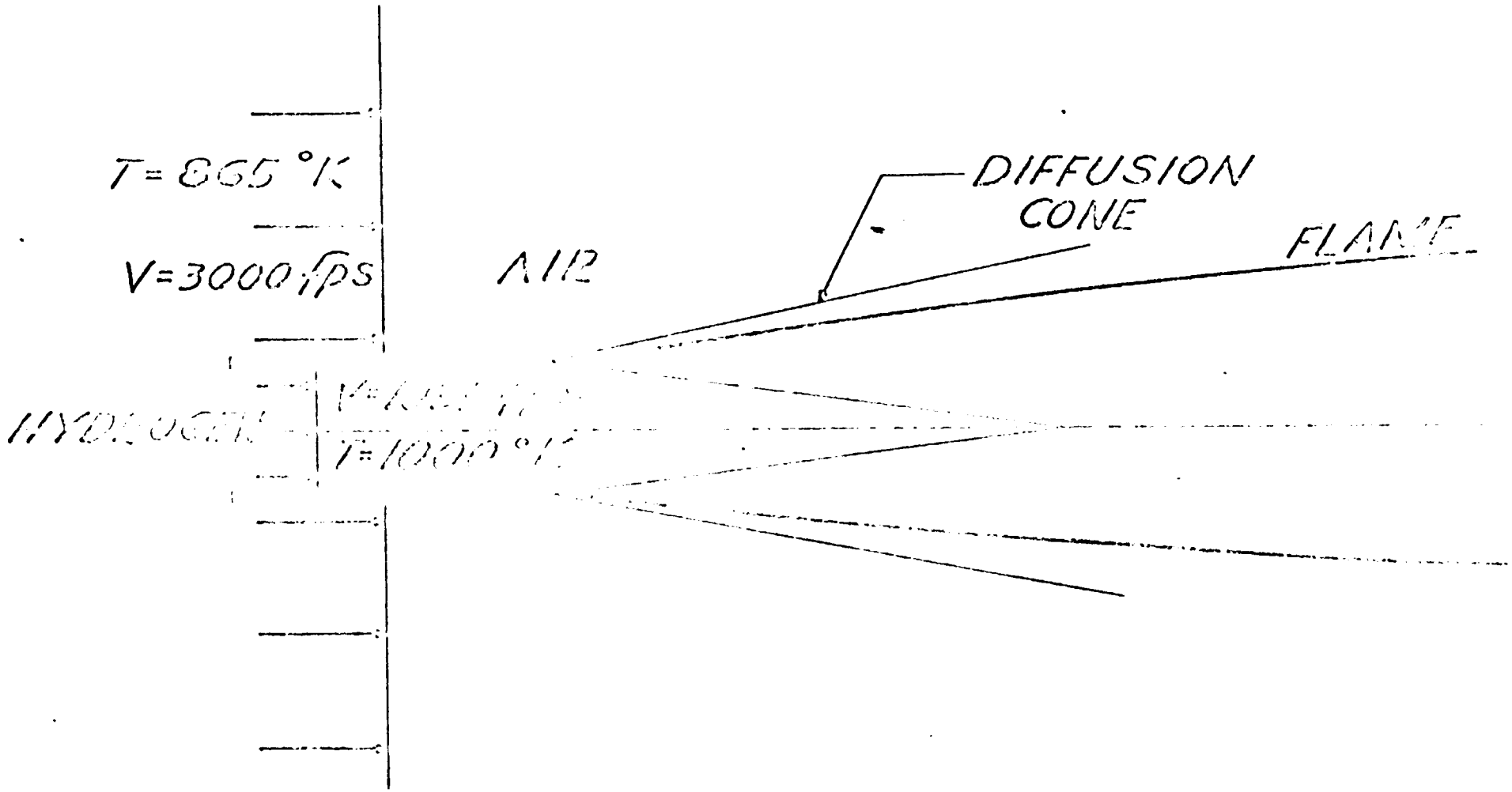

Fig. 6a Schematic arrangement of hydrogen jet

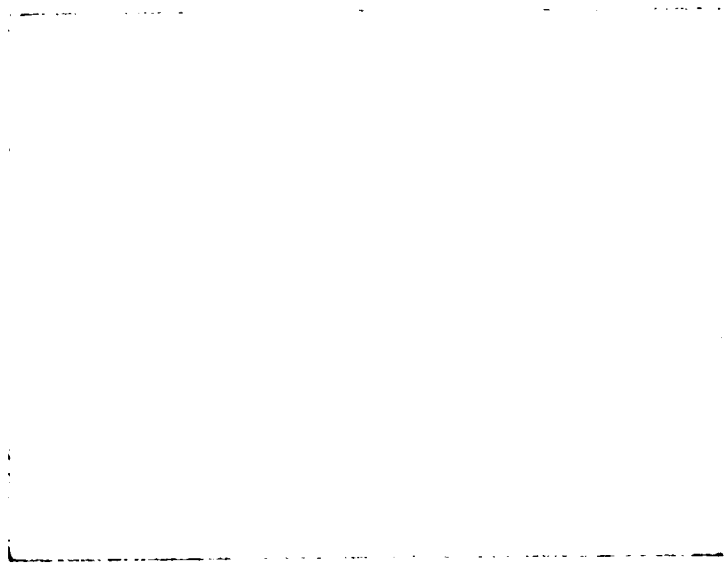

Fig. 6b Experimental flame shape for [illegible] jet

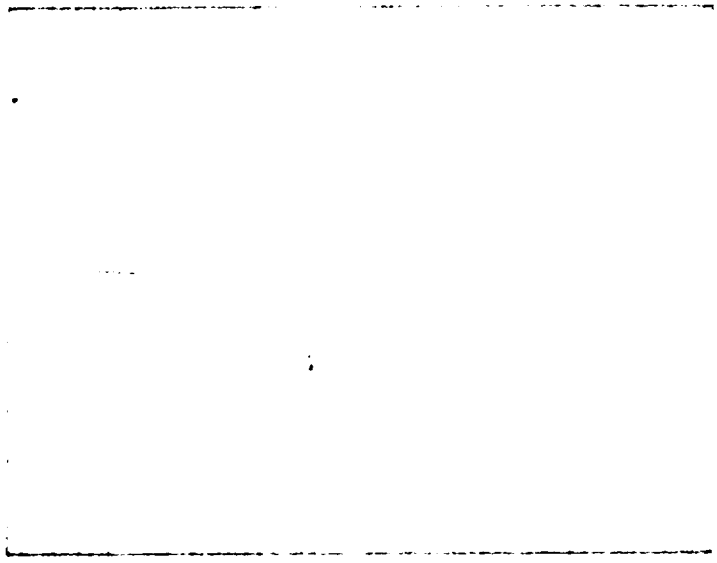

Fig. 7b Experimental flame shape for premixed flow

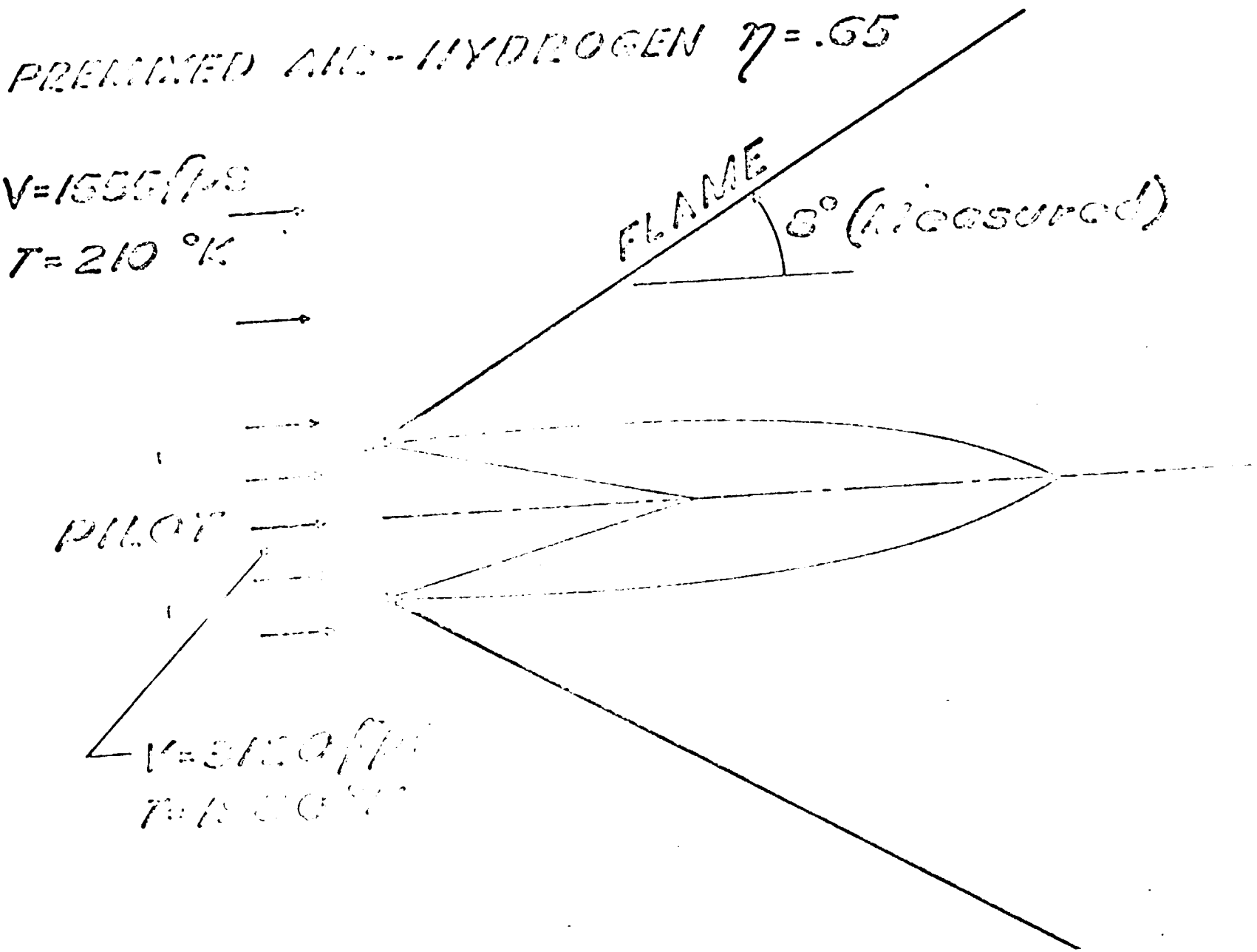

Premixed flame in premixed flow

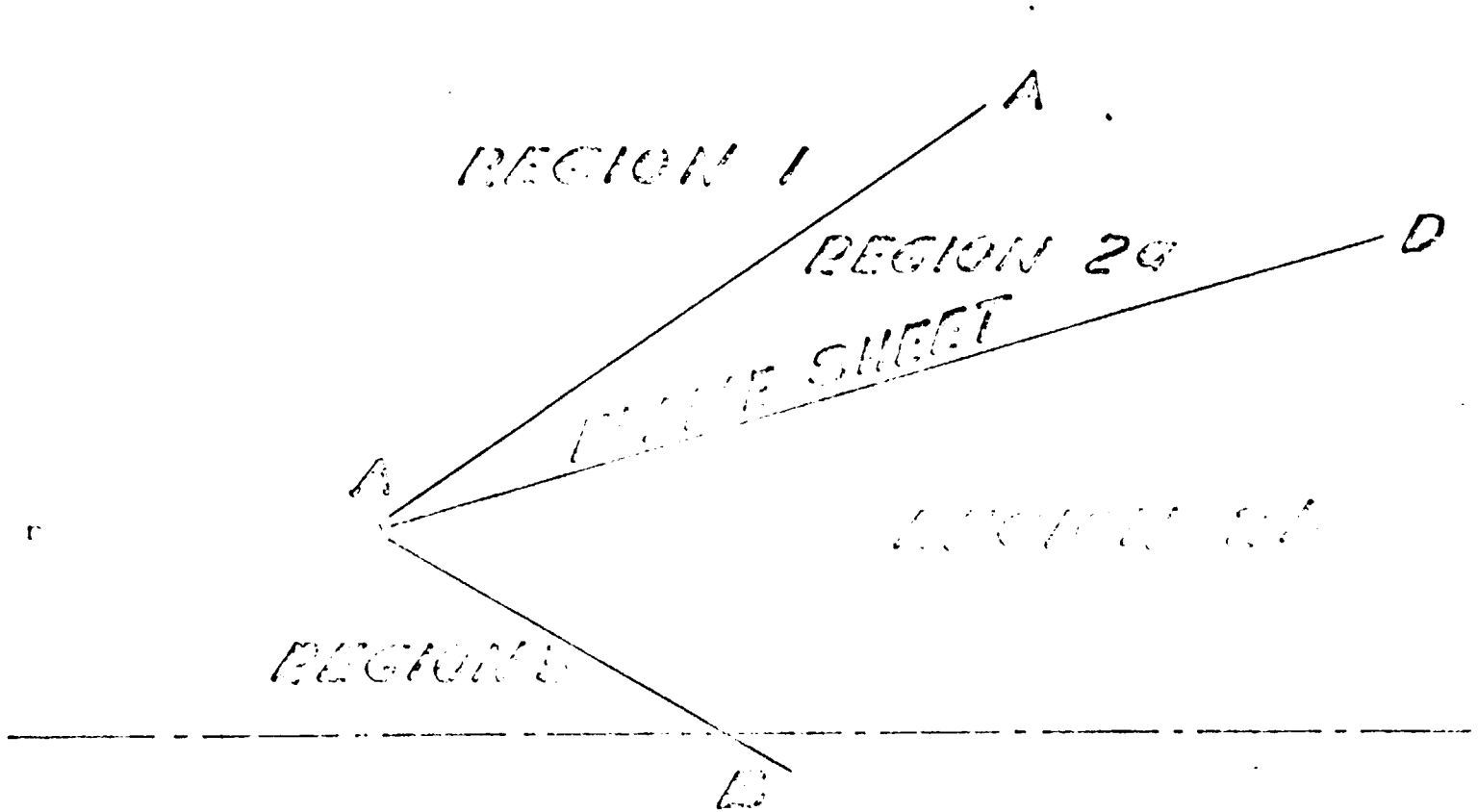

Fig. 8 Mixing in a two dimensional or axisymmetric jet flow

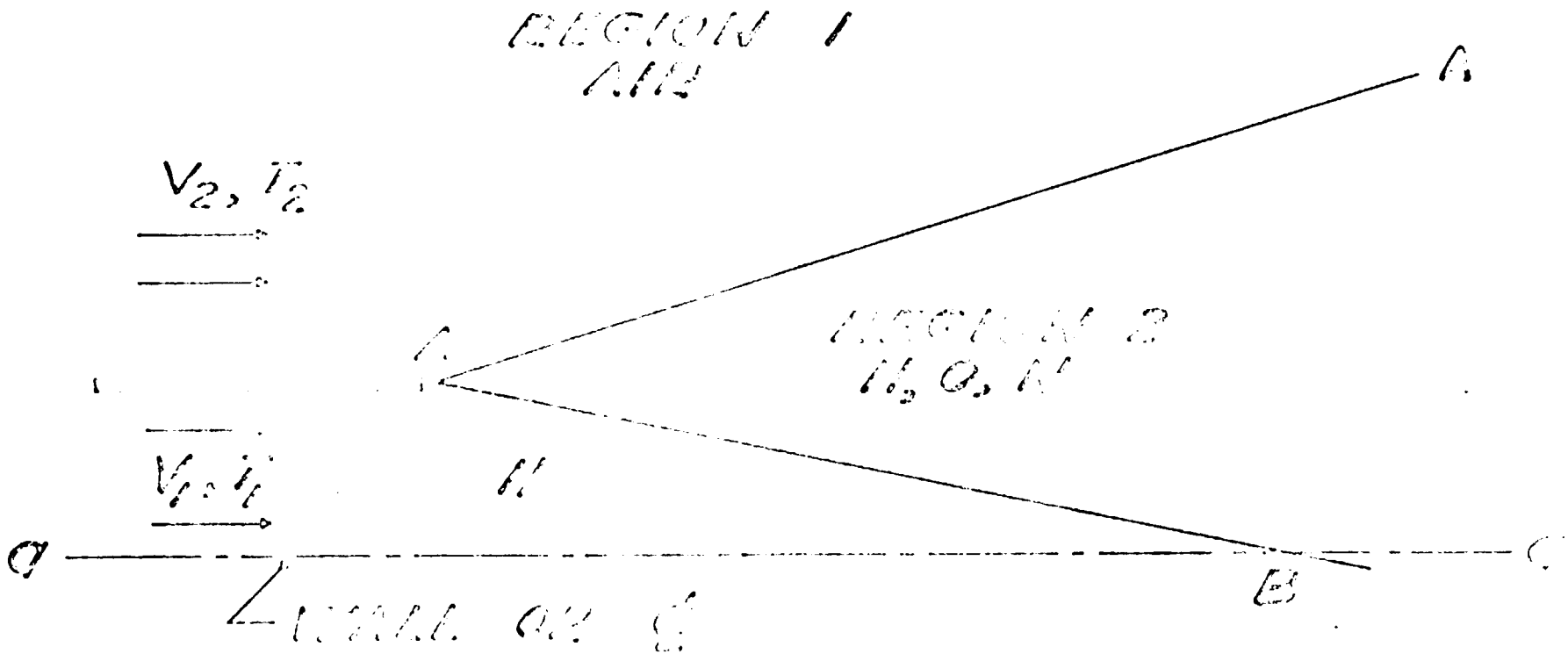

Fig. 9 Flow regions in the plane of a combustion model

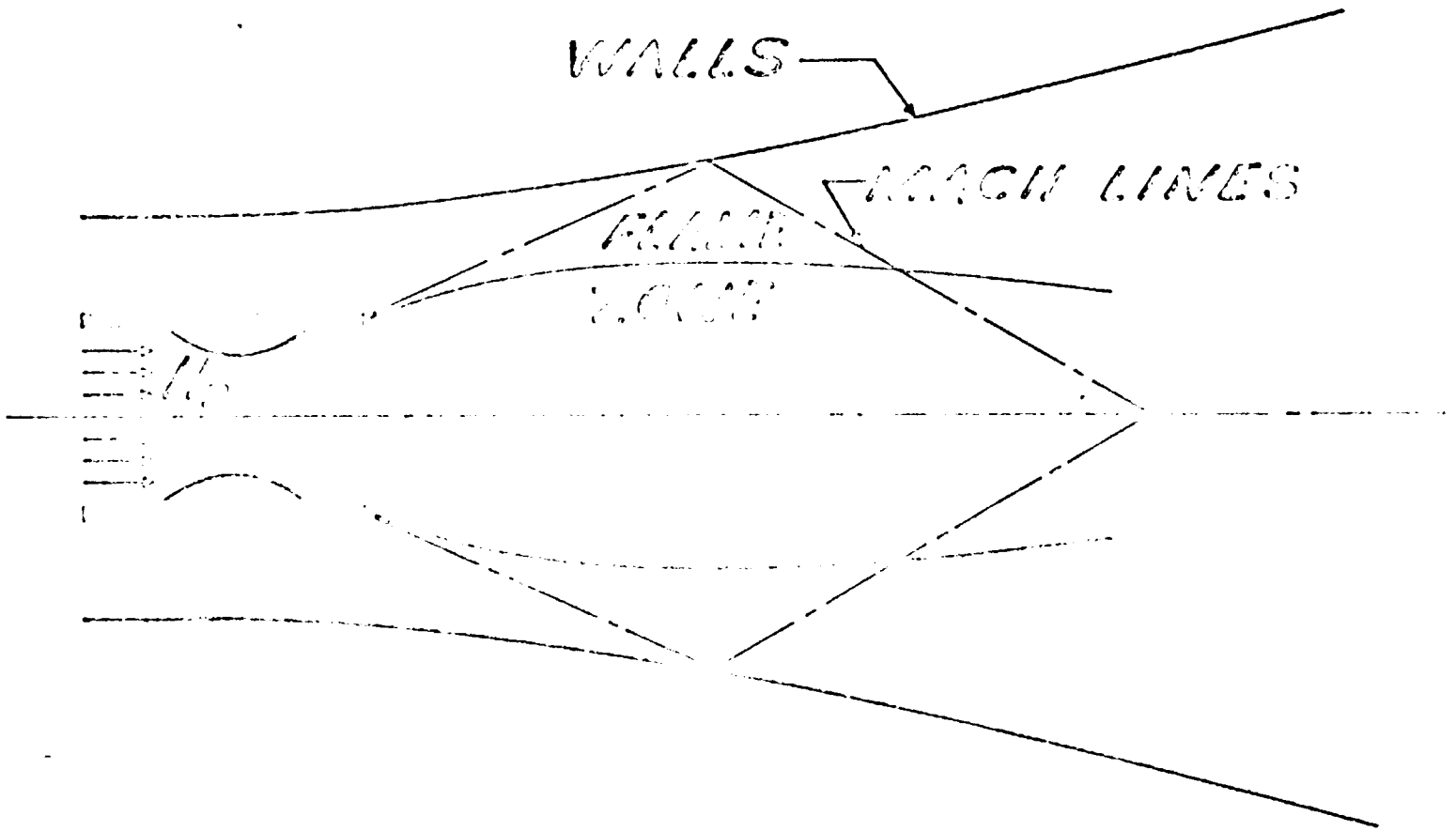

Fig. 10 Pressure interaction [illegible] flow

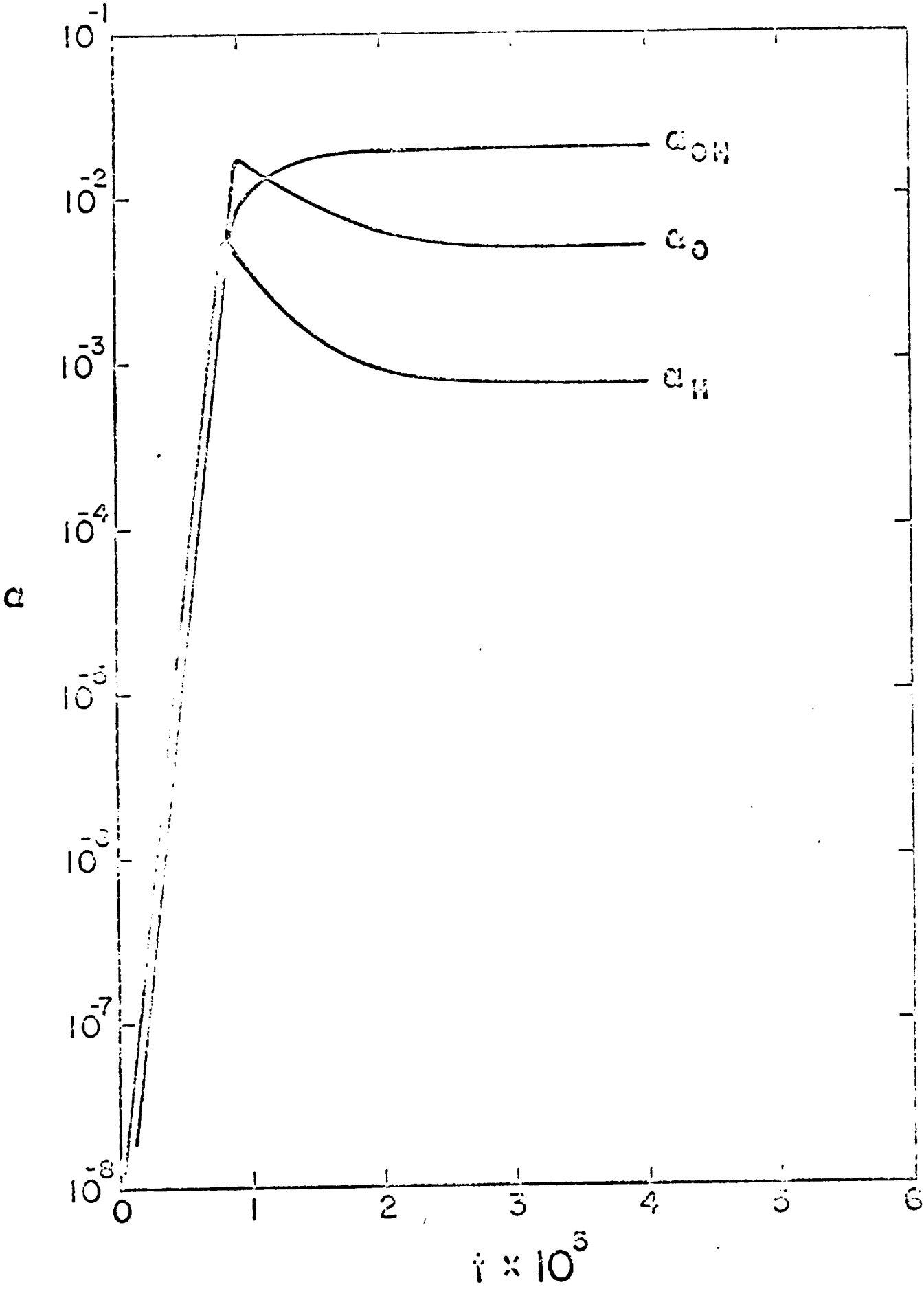

Fig. 11 Exponential time dependence of mass fractions

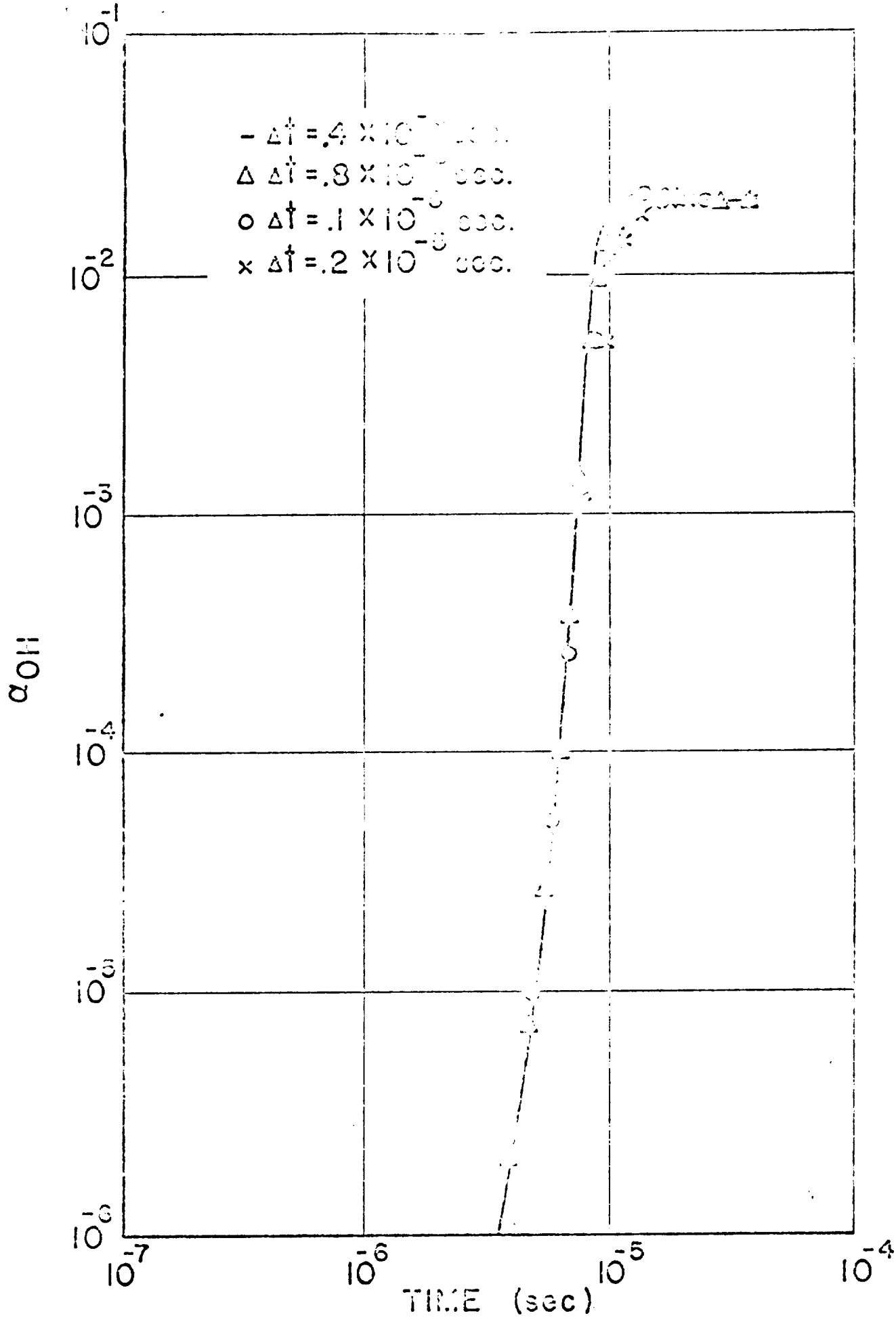

Fig. 12 Variation of accuracy with step size

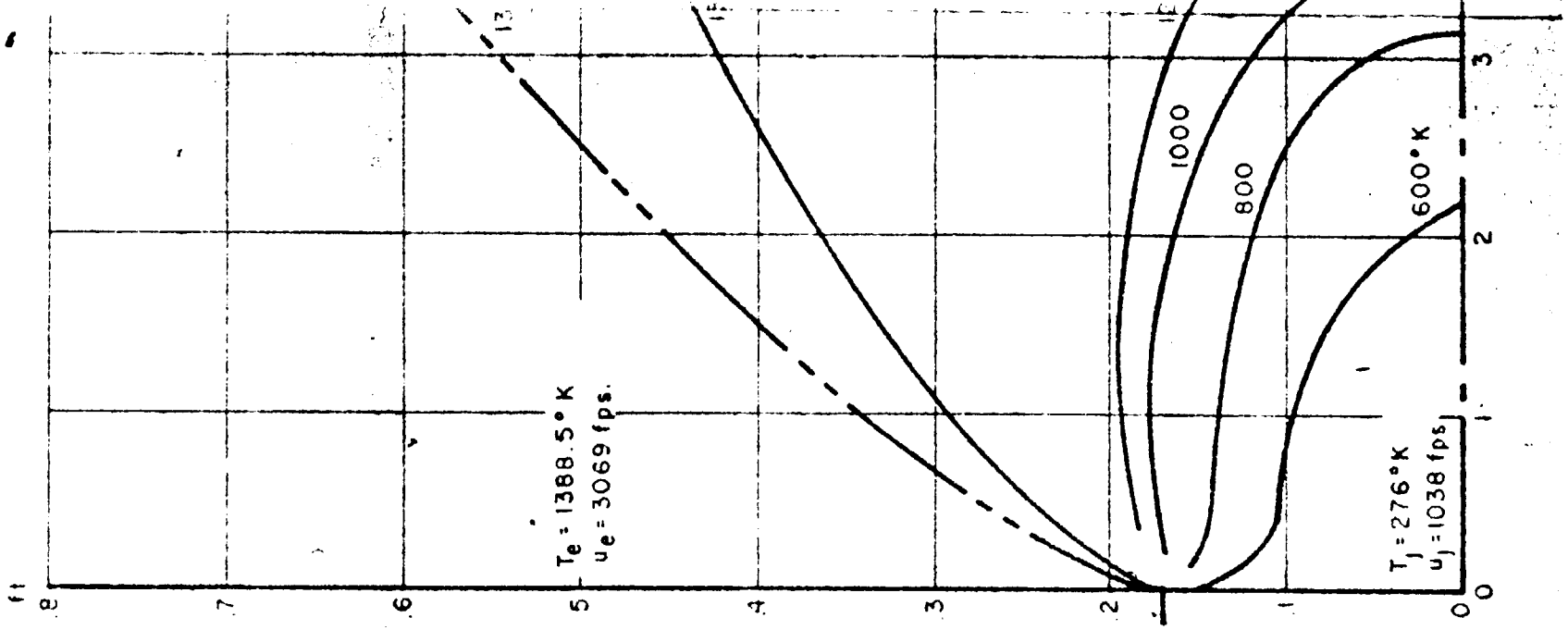

Fig. No. 13 Temperature distribution for cold jet in hot exterior air flow

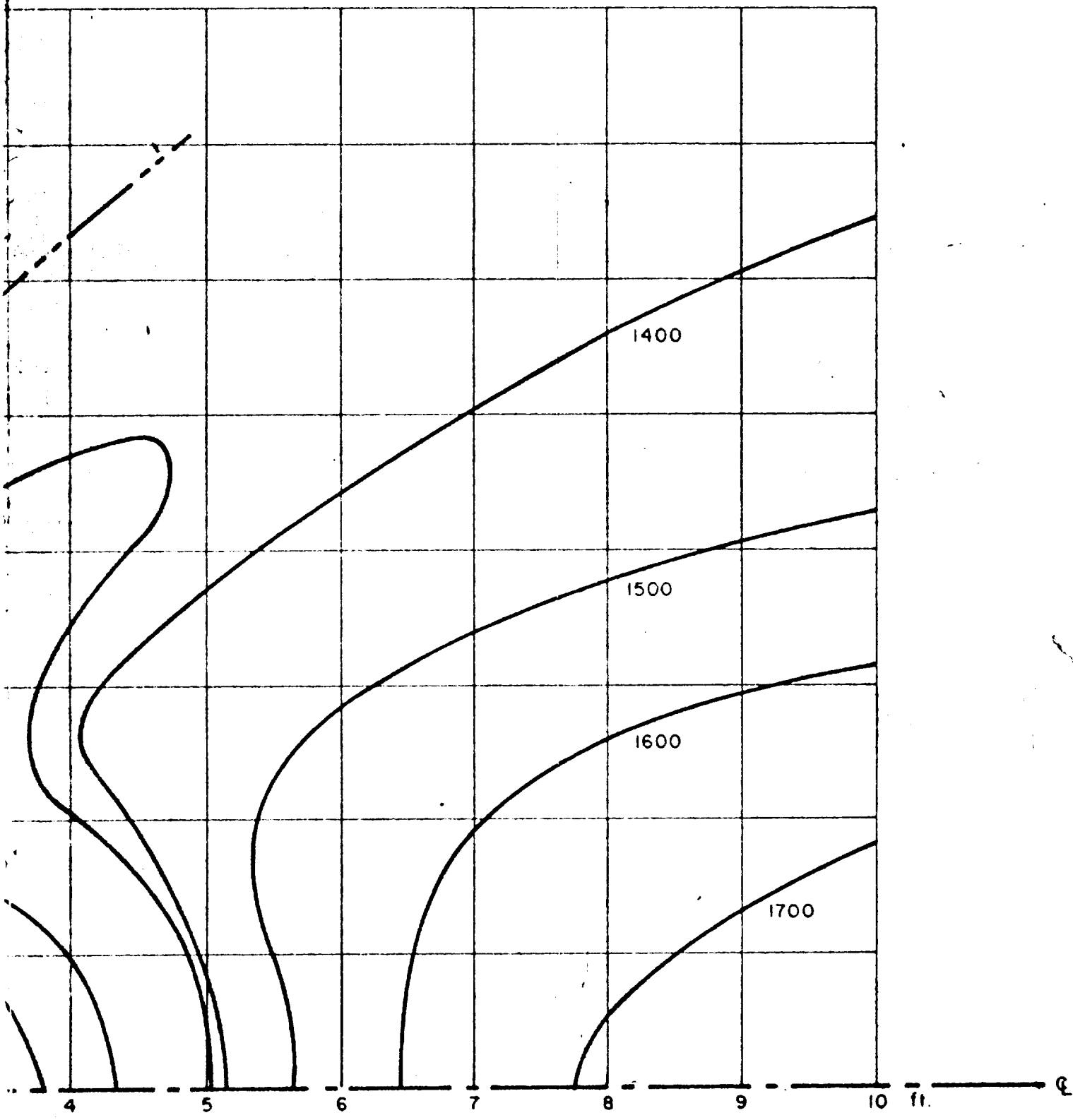
1400
1500
1600
1700
4
5
6
7
8
9
10
ft.
℄

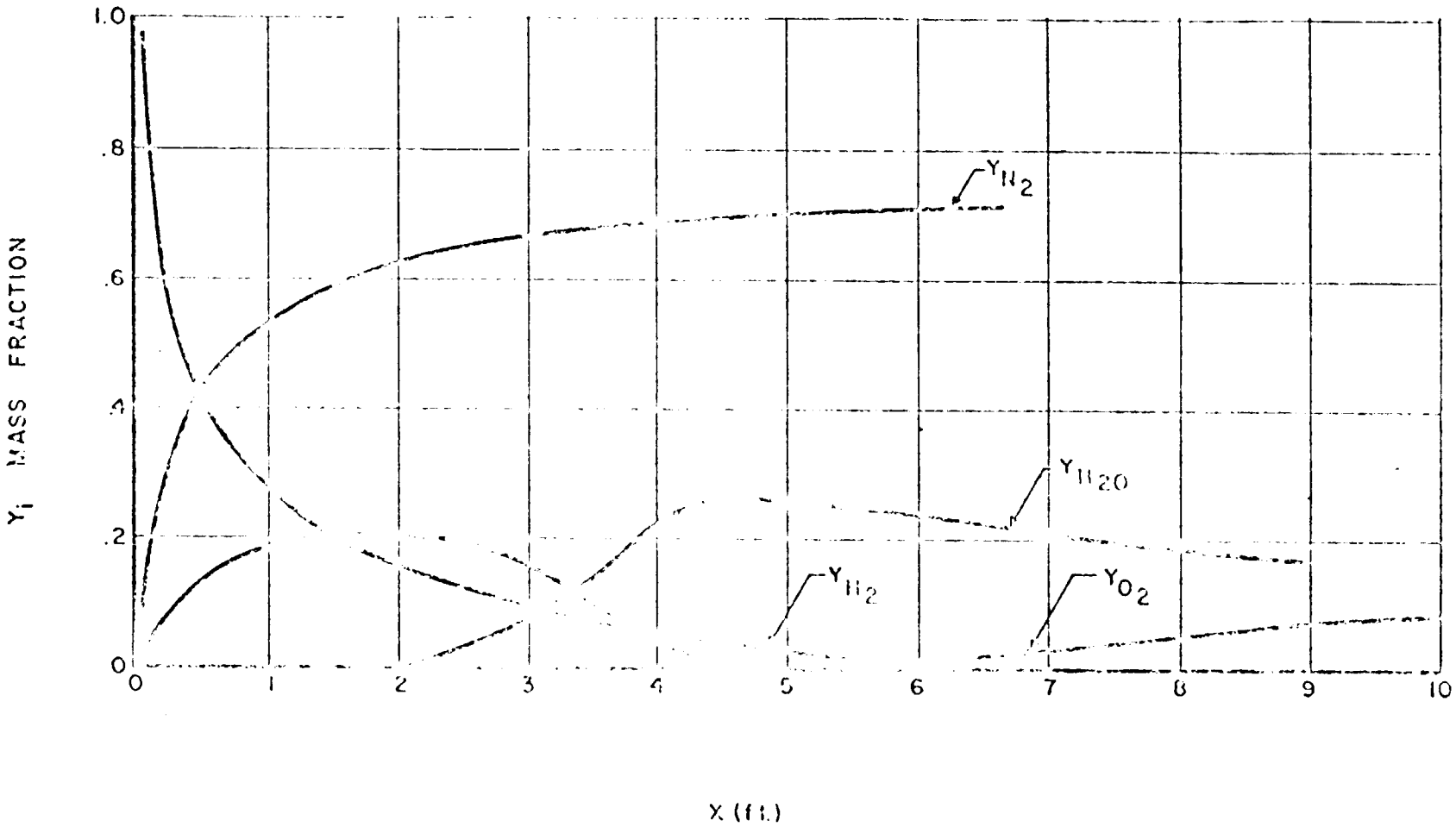

Fig. 14 Centerline concentration of hydrogen, oxygen, nitrogen and water

$T_{0c} = 1300\ ^\circ K$ $\alpha = 0.3^\circ$

$T_{0j} = 1000\ ^\circ K$

$M_c = 1.546$

$U_j / U_c = 0.349$

$\lambda = 0.022$

CALCULATED

a) MEASURED PRESSURE DISTRIBUTION

b) CONSTANT PRESSURE, $P_e = 0.32\ P_{0c}$

c) CONSTANT PRESSURE, $P_e = 0.24\ P_{0c}$

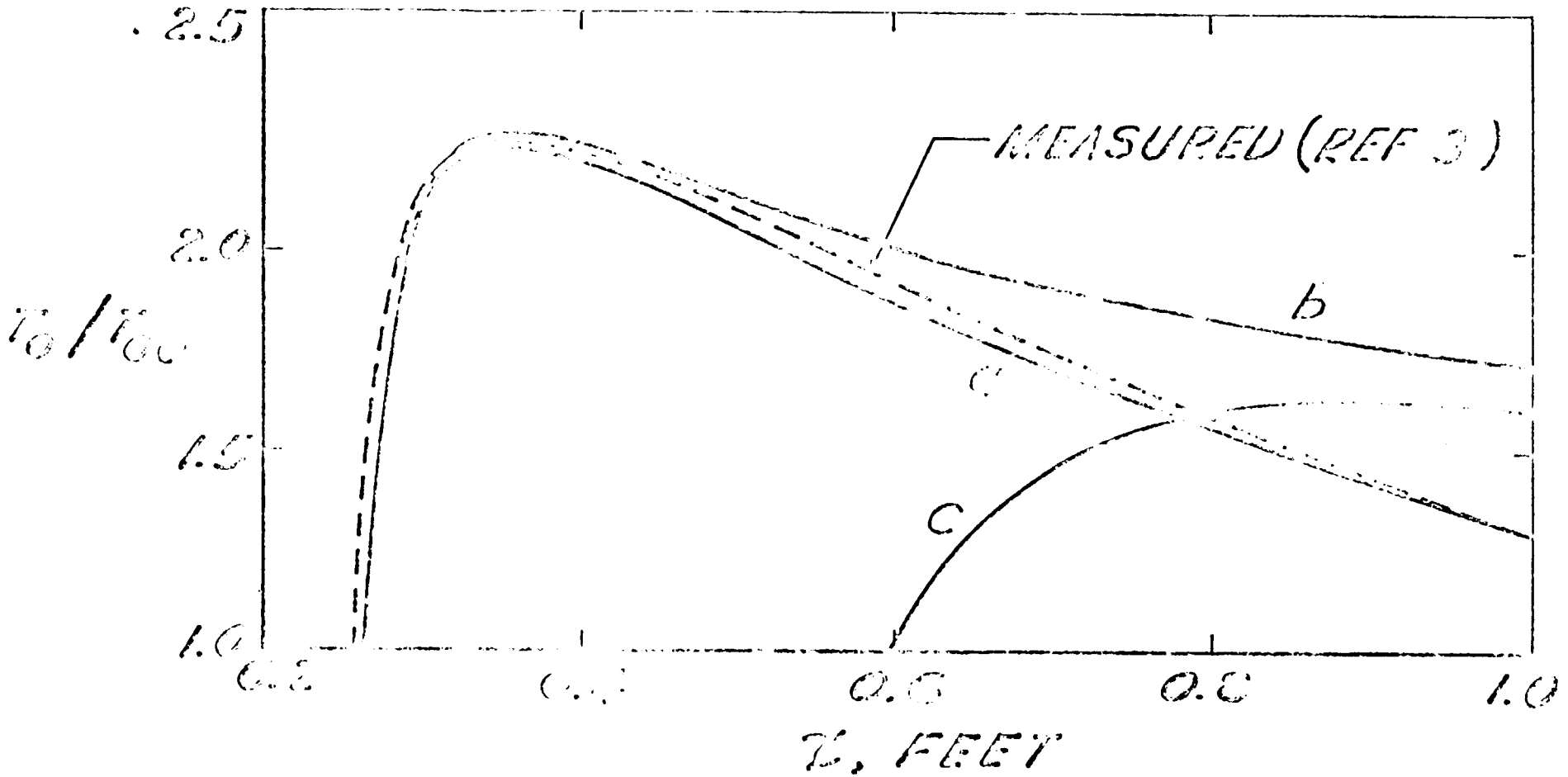

Fig. 15 Centerline temperature variation for several pressure distributions

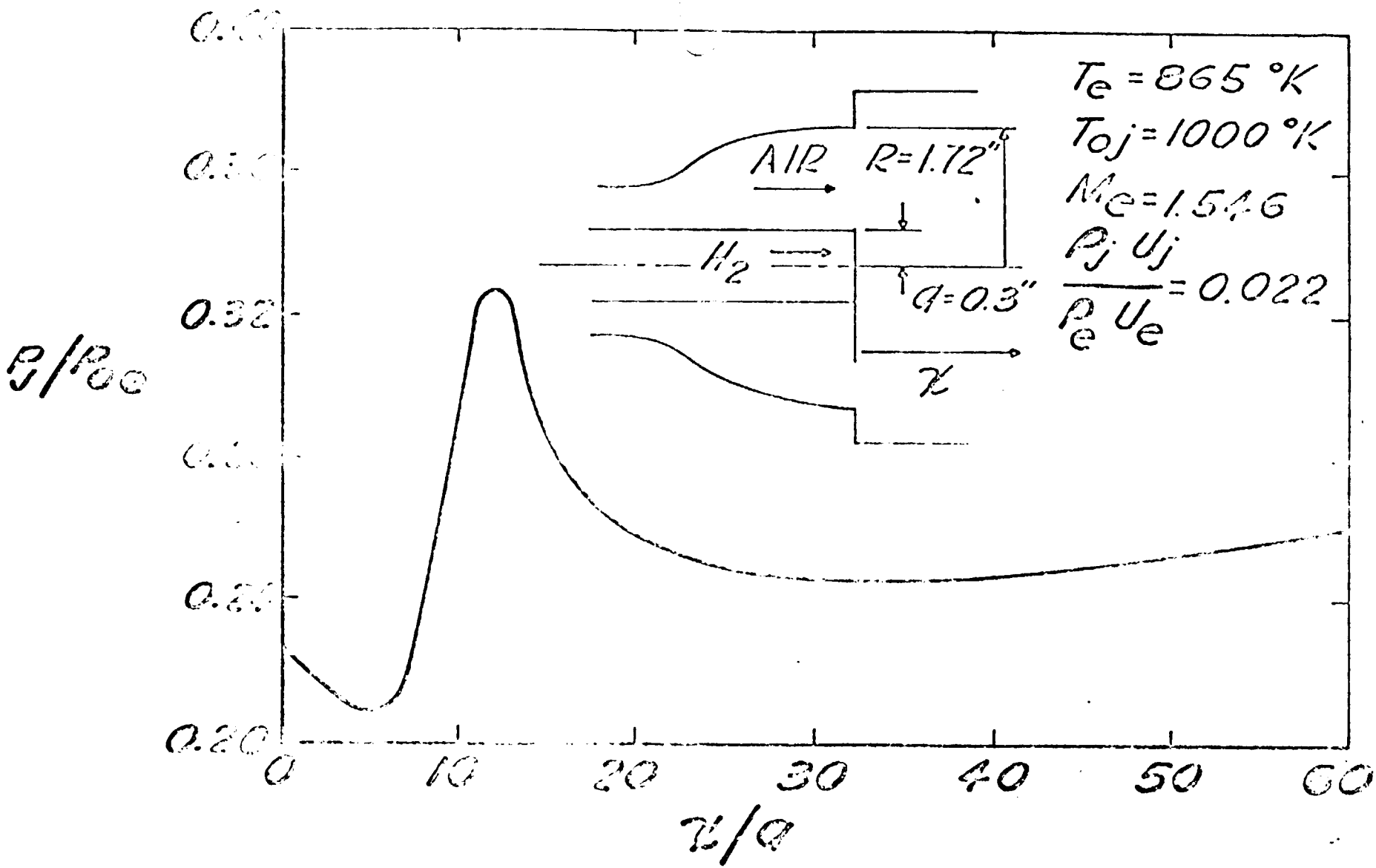

Fig. 16 Measured centerline static pressure distribution

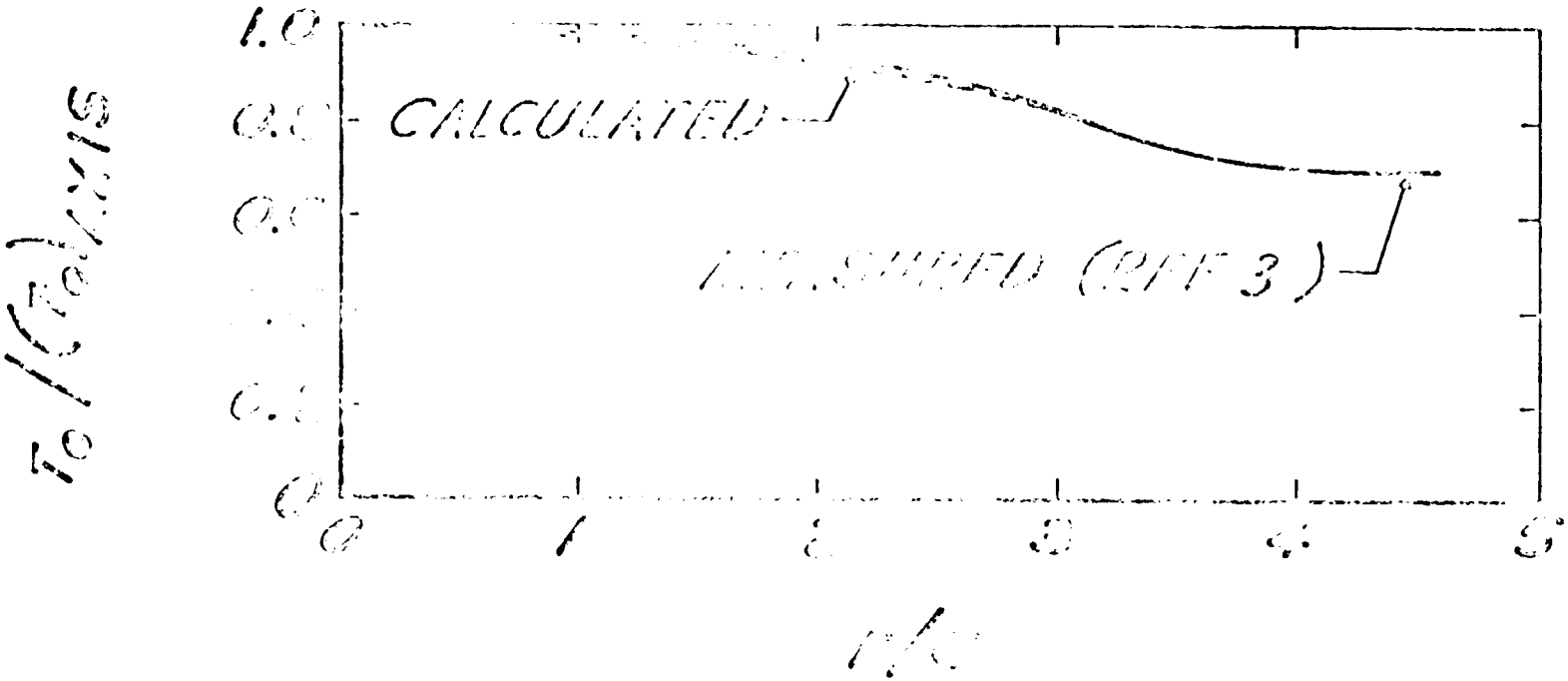

Fig. 17 Comparison of theoretical and experimental radial temperature distribution at section x=0.9 feet

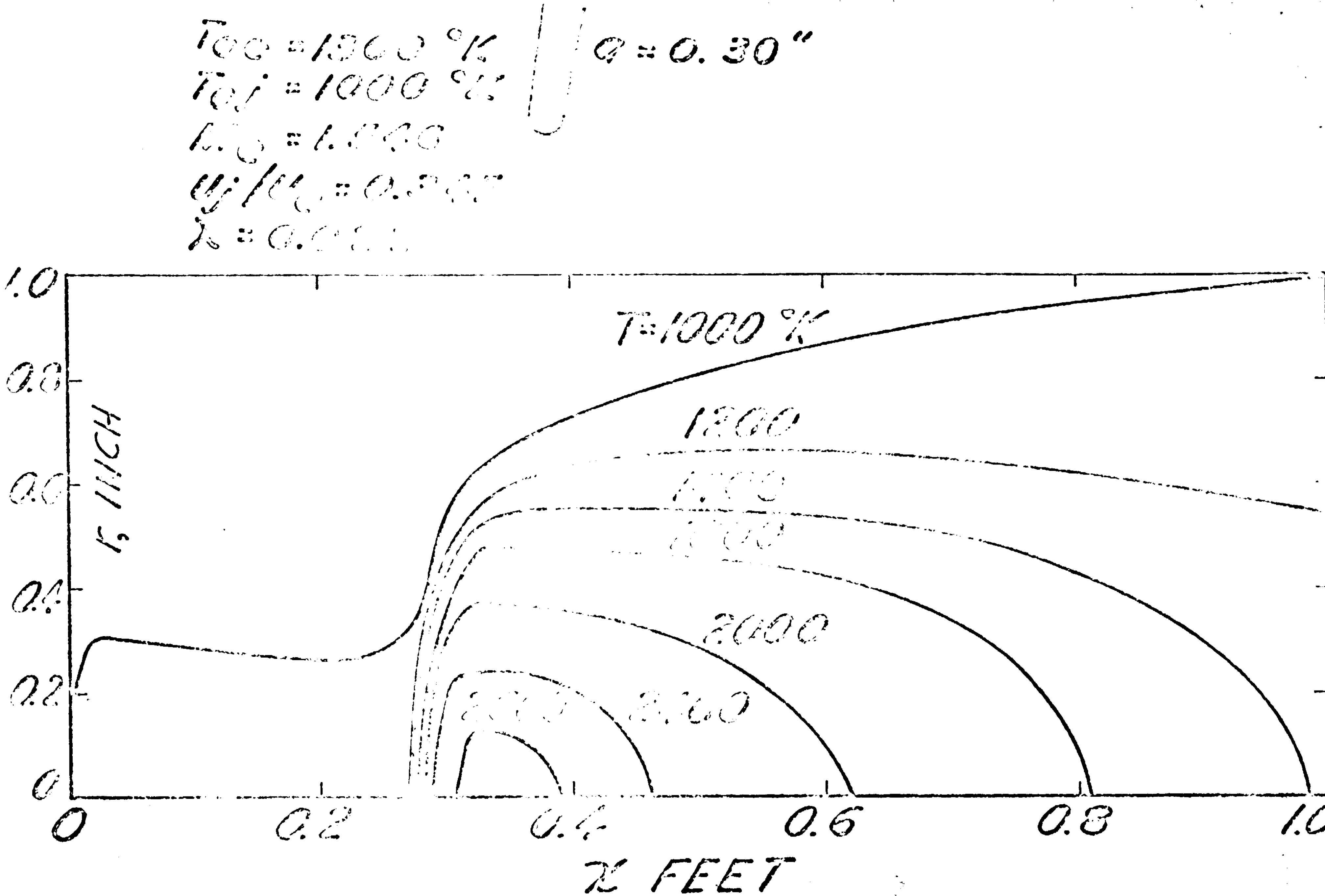

Fig. 18 Calculated isotherm map for measured centerline pressure distribution

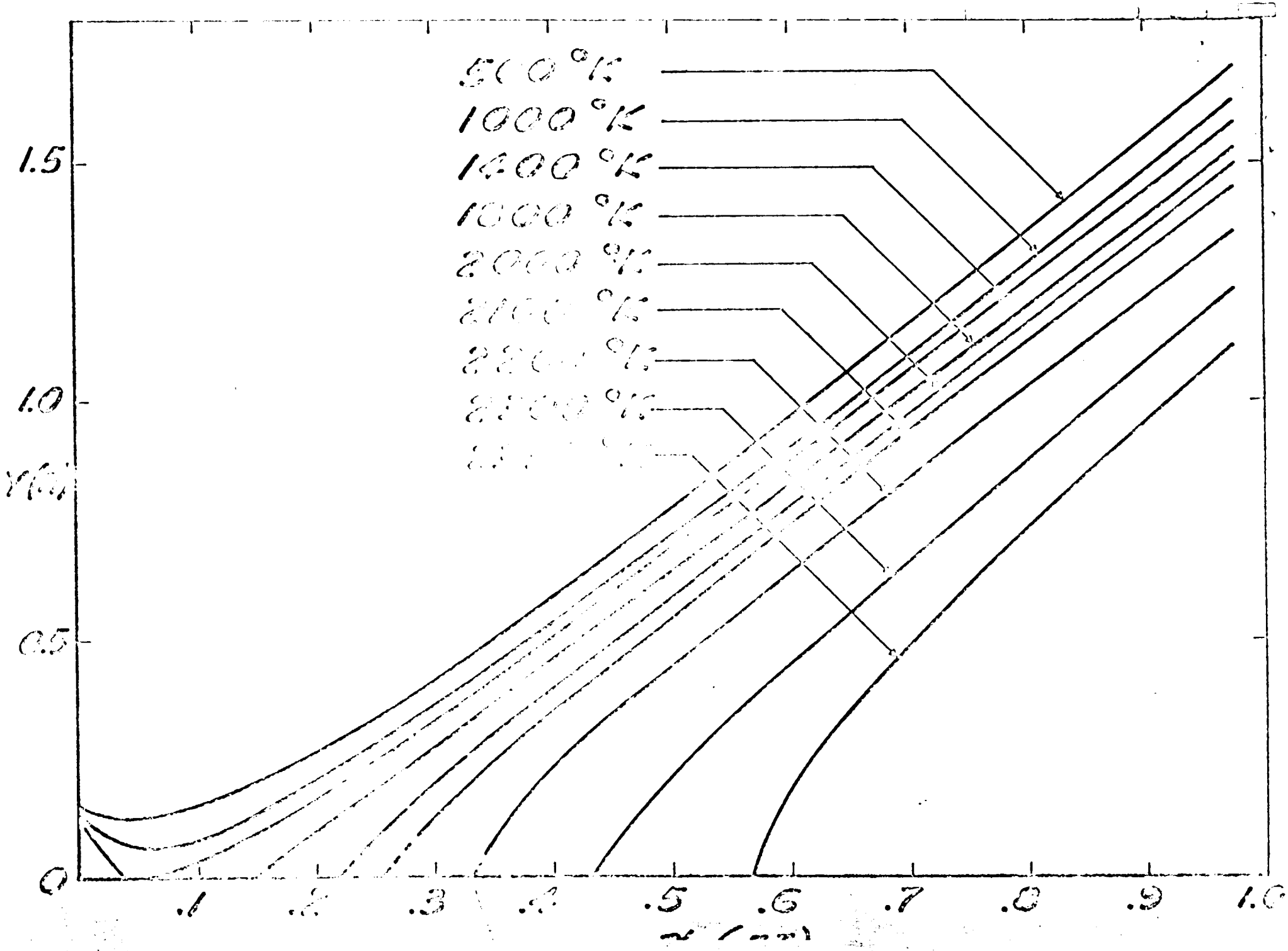

Fig. 19 Isotherm map for fl[illegible] premixed stoichiometric hydrogen flow

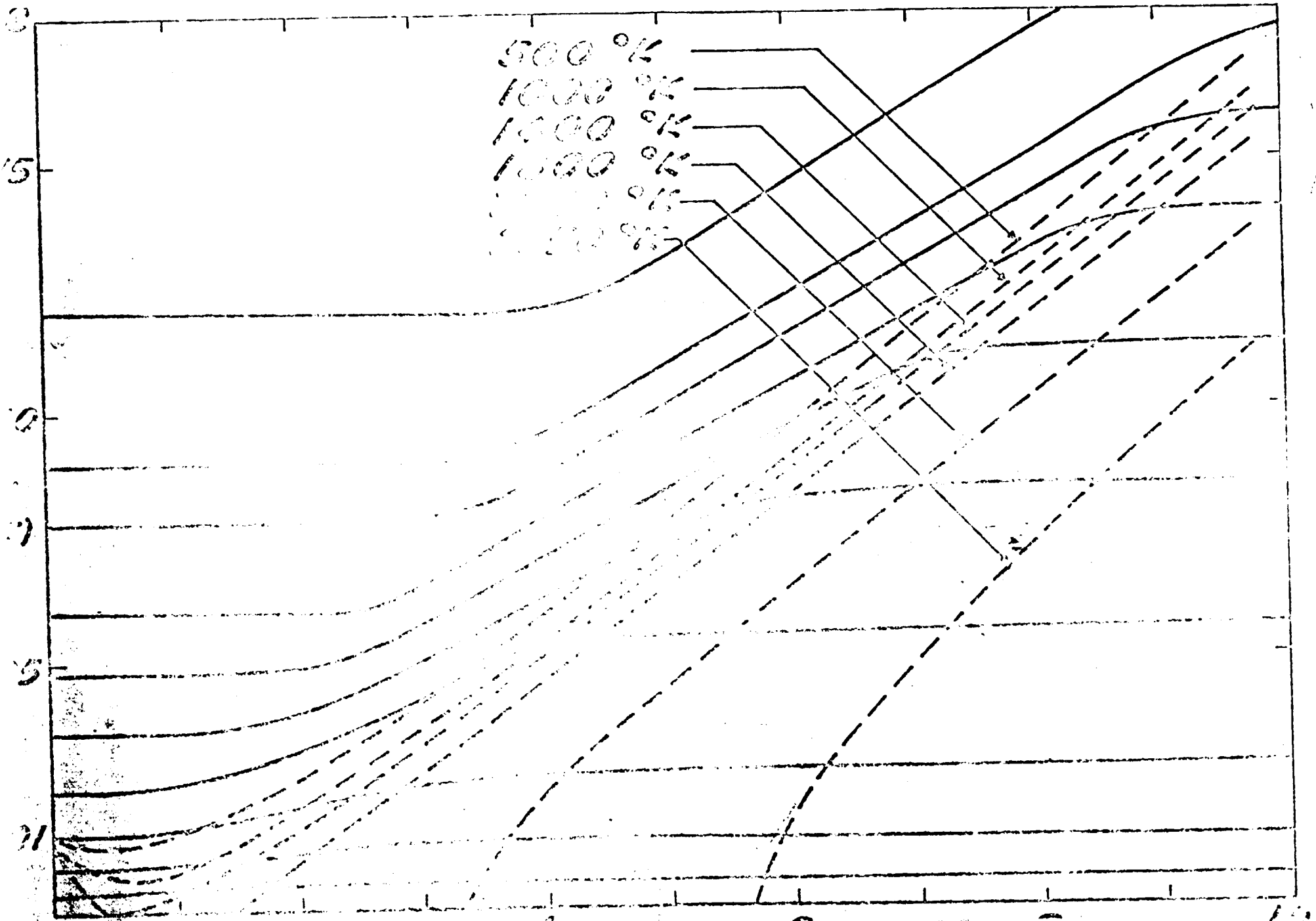

Fig. 20 Streamline map for flame in premixed stoichiometric hydrogen flow.